Ph.D. DISSERTATION

MICROWELL-BASED QUANTITATIVE GENE EXPRESSION ANALYSIS FOR SINGLE-CELL APPLICATIONS

단일 세포 유전자 발현 분석을 위한 미세우물구조 기반의 유전자 정량 분석 구현

BY

JUNHOI KIM

AUGUST 2013

DEPARTMENT OF ELECTRICAL ENGINEERING AND COMPUTER SCIENCE
COLLEGE OF ENGINEERING
SEOUL NATIONAL UNIVERSITY

Ph.D. DISSERTATION

MICROWELL-BASED QUANTITATIVE GENE EXPRESSION ANALYSIS FOR SINGLE-CELL APPLICATIONS

단일 세포 유전자 발현 분석을 위한 미세우물구조 기반의 유전자 정량 분석 구현

BY

JUNHOI KIM

AUGUST 2013

DEPARTMENT OF ELECTRICAL ENGINEERING AND COMPUTER SCIENCE
COLLEGE OF ENGINEERING
SEOUL NATIONAL UNIVERSITY

MICROWELL-BASED QUANTITATIVE GENE EXPRESSION ANALYSIS FOR SINGLE-CELL APPLICATIONS

단일 세포 유전자 발현 분석을 위한 미세우물구조 기반의 유전자 정량 분석 구현

지도교수 권 성 훈

이 논문을 공학박사 학위논문으로 제출함

2013 년 4 월

서울대학교 대학원

전기컴퓨터 공학부

김 준 회

김준회의 공학박사 학위논문을 인준함

2013 년 6 월

위 원 장 : 박 영 준

부위원장 : 권 성 훈

위 원 : 서 종 모

위 원 : 박 웅 양

위 원 : 한 원 식

Abstract

In this dissertation, a development of a low-cost and high-throughput single-cell gene expression analysis method is presented. Although the cells are fundamental building block of all living organisms, most of the studies on cell biology have only been achieved on the basis of the collective behavior of large cell populations mainly due to the challenges and limitations in analytical technologies. For this reason, some researches have longed for an improved technology enabling a reliable single-cell-level analysis and they include a study on the heterogeneity of cellular characteristics and an in-depth study on rare cells such as circulating tumor cells and cancer stem cells. Single cell analysis has therefore attracted a great attention and a development of a single cell analysis method addressing important issues in the field of biological and medical sciences is required.

Gene expression profiling, which measures level of cellular gene expressions, provides a picture of functional states of cells of interest, reflecting both intracellular and extracellular environments. By virtue of the capability of reporting temporal and spatial status of cellular functions, gene expression profiling is considered to be a powerful method for understanding complicated cellular behaviors depending on intrinsic cellular characteristics as well as extrinsic environmental factors. Gene

expression levels may differ among individual cells in a given cell population, and therefore, gene expression analysis with a single cell resolution becomes an important concern in its applications.

Here, a new methodology enabling quantification of single-cell gene expression is proposed and developed. In chapter 1, overall guidelines for dissertation are explained. Chapter 2 introduces a background and a motivation of the proposed approach utilizing a number of volume-adjusted microwells for high-throughput single-cell RT-qPCR (Reverse-Transcription quantitative Polymerase Chain Reaction).

In chapter 3 and 4, two major technical challenges for achieving a microwell-based single-cell RT-qPCR system are discussed respectively. Chapter 3 demonstrates a development of the microwell-based on-chip PCR platform enabling small volume PCR. The development of small-volume on-chip PCR system includes preparation of microwell arrays, implementation of a real-time PCR equipment, and their application for the realization of small volume PCR. Chapter 4 describes the determination of single-step lysis-RT-PCR condition realized within a fixed reaction volume. The obtained RT-PCR reagent condition enables direct cell-lysis followed by RT-PCR reaction within a single microwell with fixed reaction volume.

A detailed discussion on the multivolume microwell array approach is dealt with in Chapter 5. Single cell trapping and subsequent confinement assisted by

volume-adjusted microwell arrays are demonstrated. The integration of real-time small-volume on-chip PCR system and ‘one-pot’ lysis-RT-PCR conditions is also demonstrated. Quantification of single-cell gene expression is finally performed using the integrated single-cell RT-qPCR system.

The multivolume microwell array approach is expected to serve as a quantitative analysis system for single-cell gene expression analysis with low cost and high throughput. In addition to realizing the utilization of single-cell RT-qPCR in personalized medicine applications, the microwell-based single-cell analysis system is also expected to be further improved toward single-cell whole transcriptome analysis platform in combination with the use of DNA microarray technology and DNA sequencing technologies.

Keywords: Single cell analysis, RT-qPCR, microwell array, gene expression profiling, transcriptome analysis

Student Number: 2007-23016

Contents

List of Figures

List of Tables

Chapter 1

Introduction

In this dissertation, a development of a low-cost and high-throughput single-cell gene expression analysis method is presented. By identifying and resolving technical challenges involved in the realization of the required specifications, a new methodology enabling quantification of single-cell gene expression is proposed and developed.

In chapter 2, a background of the research and the corresponding research motivation are briefly introduced. On the basis of conventional methods for single cell handling and quantitative gene expression analysis, a new concept of single cell gene expression analysis platform employing a multivolume microwell array is proposed.

The following chapters present a development and a validation of the proposed system. To realize a microwell-based single-cell RT-qPCR (Reverse-Transcription quantitative Polymerase Chain Reaction) system, two major technical challenges should be addressed — one is the development of the microwell-based on-chip PCR platform enabling small-volume PCR reactions and the other is the determination of single-step 'one-pot' lysis-RT-PCR condition realized within a fixed reaction volume. By overcoming those technical problems and combining their solutions, an integrated single cell gene expression analysis system has been developed.

In chapter 3, a development of a microwell-based on-chip PCR system is described. A microwell array microchip with a number of microwells serving as isolated small-volume reaction chambers is designed and prepared for performing PCR reactions. An automated real-time on-chip PCR monitoring system is also developed in order to acquire quantitative PCR results from the microchip. Using a simple model PCR reaction, the developed microwell array environment and its application to PCR reaction are validated.

In chapter 4, a variety of different RT-PCR conditions were investigated for the purpose of the realization of 'one-pot' lysis-RT-PCR. To be adopted to the microwell configuration, an exquisite RT-PCR reagent condition should be obtained to allow direct release of intracellular RNA from cells and subsequent RT-PCR reactions within a fixed reaction volume. After a series of experimental investigations, a RT-

PCR reagent condition employing intact cell samples as a target for direct amplification is successfully determined.

In chapter 5, the integration of the two — small-volume on-chip PCR system and ‘one-pot’ lysis-RT-PCR conditions — achievements toward single-cell RT-qPCR is described. To achieve a capability of single cell gene expression analysis, a multivolume microwell array employing two pairing microwells, each of which has different microwell volume, is suggested and prepared. After the integrated system is validated through conventional RT-qPCR analysis, quantitative analysis of single cell gene expression is performed. The achieved system is expected to serve as a quantitative analysis system for single cell gene expression profiling with low cost and high throughput. The microwell-based single cell analysis platform can also be further improved toward single-cell whole transcriptome analysis in combination with the use of DNA microarray technology and DNA sequencing technologies.

Chapter 2

Background and Motivation

This chapter introduces a background and a motivation of this dissertation. After presenting the necessity for single cell analysis, a series of analytical methods for single cell analysis are briefly introduced. Among various cellular analyses, quantitative gene expression analysis is especially considered for single cell applications in biological and medical sciences. On the basis of the previously-established approaches for quantitative gene expression analysis, a main concept of a multivolume microwell array for single cell gene expression quantification is finally introduced.

2.1 Why Single Cell Matters

Cell is the fundamental unit of all known living organisms in terms of structure and function. Although the cells are basic building block of life, most of the studies on cell biology have only been achieved on the basis of the collective behavior of large cell populations mainly due to the challenges and limitations in analytical technologies. For this reason, some researches long for an improved technology enabling single-cell-level analysis and thereby preventing particular single-cell signals from averaging out to characterless ones. For instance, some researches focusing on the heterogeneity of cellular characteristics require distinguishment of individual cells for the desired analysis. Also, some other researches seeking in-depth studies on rarely-distributed cells out of an abundant cell population demand high sensitivity of analysis at the single cell level. In short, single cell analysis has attracted a great attention due to its capability of enabling quantitative analysis on the fundamental unit of biology [1-6].

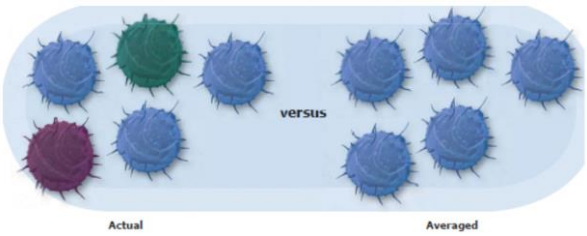

Figure 2.1 A conceptual view of heterogeneous cellular distribution and its appearance determined by the collective studies.

2.2 Single Cell Analysis Methods

A basic difficulty in single cell study is to pick a single cell for the desired analysis. Because of its small size (~ 20μm in diameter), specialized cell-handling skills are required in order to ensure that only one (not two or more) cell is being involved during the analysis. One simple approach would be a limiting dilution, which successively dilutes a cell suspension until a given sample contains a single cell only. After sufficient dilutions a series of diluted samples are considered to have a probability that contains a single cell following Poisson distribution. This statistical approach ensures obtaining of samples having a single cell out of a number of the diluted samples; however, it is not certain whether each diluted sample contains a single cell or not until the analysis result comes out. Also, the concentration of the cell or its sub-compartments is inevitably very low, making its analysis challenging due to the low sensitivity.

Handling of single cells using a micromanipulator would be an alternative option [7, 8]. The use of micromanipulator under microscopic observation ensures that a single cell of interest truly participates in the analysis. However, the process is very labor-intensive and the throughput of picking single cells is extremely low. Highly-developed technologies with high throughput have also been used in single cell studies and one of the good examples is fluorescence-activated cell sorting technologies [9, 10]. The automated cell sorting enables the preparation of a number

of single cells in the separated reaction chambers. However, the whole system is so bulky and expensive that only a limited range of applications is allowed. For instance, its tremendous technical capability cannot be utilized in the personalized medicine applications due to its extremely high fixed and operating cost.

Microfluidics devices and lab-on-a-chip technologies also provide the capability of single cell analysis [11-17]. By virtue of small reaction volume compatible to the volume of a single cell, a dramatically-increased sensitivity is achievable in single cell analysis. The small reaction volumes also provide further advantages in the analysis throughput thanks to the capability of integration and parallelization. Various studies have been endeavored to enable challenging researches on single cells, and these studies have made remarkable progress in the context of increased scale of analysis and reduced cost.

2.3 Quantitative Gene Expression Analysis

Among a variety of cellular analyses in the field of molecular biology, quantitative gene expression analysis is of intense interest and has a number of applications in biological and medical sciences. In contrast to genome analysis which provides almost identical genetic information across different cells of a single entity, measuring level of cellular gene expression gives a picture of functional states of cells of interest, reflecting both intracellular and extracellular environments. Therefore, gene expression profiling can, for instance, be used to analyze the reactive behavior of cells to a particular stimulus such as drug exposure.

To analyze gene expression levels of cells of interest, various methods have been developed and utilized. DNA microarray technology is the most common approach to measure cellular activities of previously known genes [18-23]. By immobilizing a number of different DNA strands capable of capturing target RNA transcripts, DNA microarray is designed to report the abundance of diverse target transcripts based on the number of DNA hybridizations. DNA microarray technology has been a reliable gene expression analysis method with an amount of accumulated reference information. However, it is only applicable to previously identified genes and it cannot detect the RNA transcript with low copy numbers.

Other gene quantification methods relying on the amplification of DNA are also widely used. RT-qPCR is an amplification-based quantification method with a

good sensitivity and specificity [24-27]. RT-qPCR has also a wide dynamic detection range in which a single copy of target RNA molecule can be even detected through gene-specific amplification. Digital PCR, which employs a number of separated PCR compartments, is able to count the number of gene transcript with single molecule resolution [28-30]. In contrast to RT-qPCR, precise estimation of gene expression level can be achieved by digital PCR technologies. Despite of a number of advantages of the amplification-based methods, they suffer from lack of throughput and multiplexity; the number of genes simultaneously analyzed is severely limited compared to DNA microarray.

Recently, next-generation DNA sequencing technologies reading all the genetic information of samples of interest were developed [31-38]. The utilization of DNA sequencing technologies for transcriptome analysis can not only count the number of transcript but also read out individual base information of the transcripts [39-43]. The tremendous advantages of DNA sequencing technologies have yielded unprecedented achievements; however, its analysis cost is a lot higher than other conventional approaches, restricting its usage only to limited applications.

On the other hand, advancements in microfabrication technology have led to the development of microfluidics and lab-on-a-chip technology, which in turn enabled scale-up of various methodologies in molecular biology through miniaturization and parallelization. In the area of quantitative gene expression

analysis, those innovative approaches include high-throughput digital PCR [44-47], multiplexed PCR [48-51] and single cell RT-qPCR [52, 53]. Although a large variety of methods are being utilized for quantitative gene expression analysis, a development of a new reliable method with low cost and high performance is still required; especially, a capability of high-throughput single-cell analysis is required to serve as a next-generation technology in the field of molecular biology.

2.4 Main Concept: A Multivolume Microwell Array

This dissertation presents a development of a multivolume microwell array for the application of high-throughput single-cell gene expression analysis. In contrast to the previously-demonstrated single-cell RT-qPCR platforms employing a complicated network of microfluidic channels, pumps and valves [52, 53], the multivolume microwell array technology simply employs a number of microwells as small-volume (~10nL) reaction chambers in which 'one-pot' single-cell lysis-RT-PCR reaction is performed. This high-throughput microwell-based single-cell RT-qPCR with reduced complexity is expected to enable high-throughput and low-cost gene expression profiling at single-cell level.

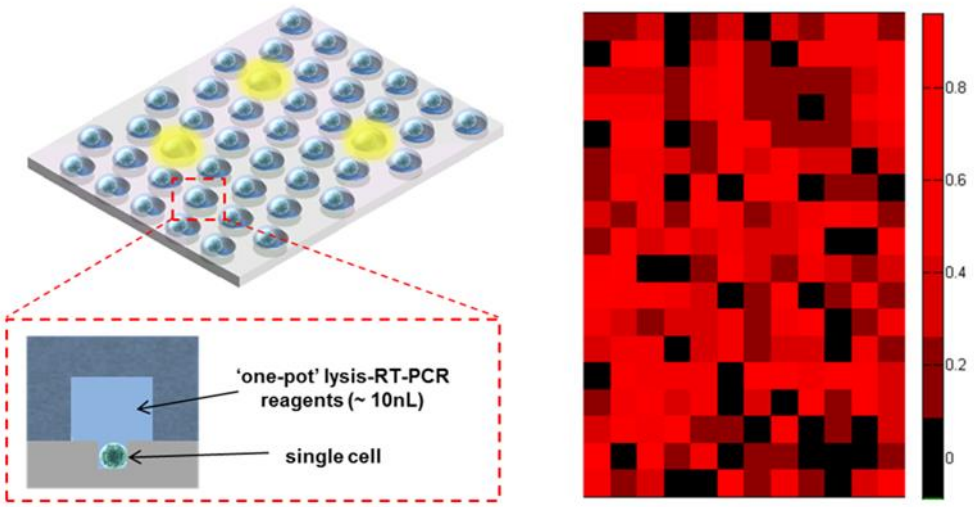

Figure 2.2 A concept of a multivolume microwell array for quantitative single-cell gene expression analysis

Chapter 3

Small Volume On-Chip PCR

To achieve a microwell-based single-cell RT-qPCR system, two major technical challenges should be overcome — one is the development of the microwell-based on-chip PCR platform enabling small volume PCR and the other is the determination of single-step lysis-RT-PCR condition realized within a fixed reaction volume. This chapter describes how small volume on-chip PCR platform was developed. This chapter deals with the technical achievements including development of a microwell array microchip, development of a real-time PCR equipment, and their application for the realization of small volume PCR.

3.1 Microwell Array Preparation

In biotechnology, microwell array technologies are simple and easily-accessible lab-on-a-chip approaches enabling high-throughput biochemical reaction analysis based on independent small volume reactions in a highly-parallelized manner [54-59]. Here, a microchip employing a large number of microwells is designed and fabricated to serve as a high-throughput small volume PCR platform. Application of the microchip to the single cell analysis is also considered.

3.1.1 Design

A microwell array was designed to have identical microwells with a volume of ~12.5nL ($w \times l \times h$ = 250μm × 250μm × 200μm) and an interwell spacing of 250μm. The volume of the single microwell was determined under the consideration of single-cell application requirements. Details of reaction volume requirements for single-cell analysis are discussed in the '5.1 Multivolume Microwell Array' section. Long and single-directional drain channels were placed between every 7 microwells (Figure 3.1) so as to drain liquid out of the microchip during the microwell sealing process. The spacing between two liquid drain channels was therefore determined to be 3.75mm which fits optical field-of-view of the microchip imaging system. Details on optical imaging setup are discussed in the next section. Under those microwell array specifications, 35 microwells can be analyzed within a single optical field-of-

view. A single microchip (~18mm × 12mm) was designed to cover 9 optical field-of-views thereby include 315 microwells in total.

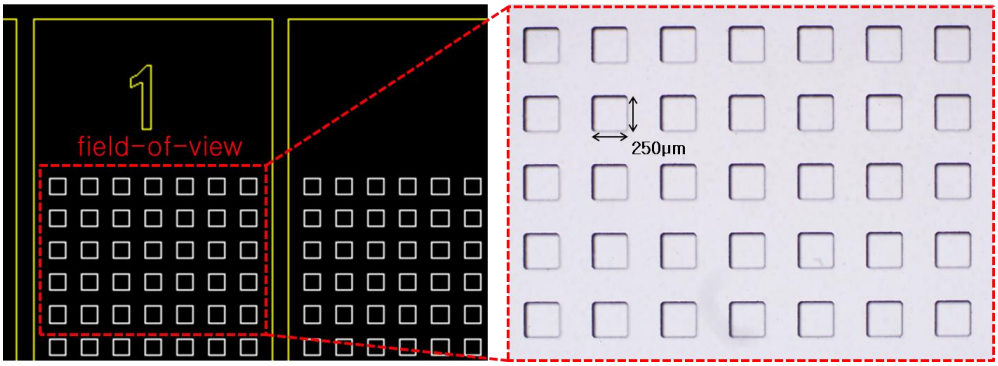

Figure 3.1 Design and fabrication of a microwell array

3.1.2 Fabrication

A microwell array microchip was fabricated through simple soft lithography technique [60]. First, pattern mold was prepared by forming SU-8 (SU-8 2150, MicroChem) micropillars onto a silicon wafer through conventional photolithography process. An elastomeric polymer — polydimethylsiloxane (PDMS, Sylgard 184, Dow Corning) — was then poured onto the pattern mold and thermally cured at 60˚C for 12h. The peeled PDMS block with microwell patterns was used as a microwell array in this research.

3.1.3 Liquid Loading and Microwell Sealing

Under the condition of complete sealing of microwells, each microwell in a single microchip functions as an isolated liquid reaction chamber, providing independent microfluidic environment. In order to achieve multiple identical reaction chambers with precisely-controlled reaction volume, all microwells should be fully filled with the liquid of interest during the sealing process. However, a simple microwell sealing approach, which simply places a flat plate on top of a microchip, often suffers from air bubble formation induced by the interaction of microchip surface and liquid unless the sealing process is performed in liquid-rich environment such as a liquid chamber. Therefore, a sophisticated handling of liquid is required to provide a reliable bubble-free liquid loading.

Here a hydrophilic/hydrophobic patterned PDMS substrate was used for reliable liquid loading (Figure 3.2). The PDMS substrate having a central hydrophilic region and an external hydrophobic region was simply prepared by partial covering of the PDMS-coated glass substrate using adhesive tape followed by oxygen plasma treatment. The loaded liquid is not spread throughout the substrate but confined in the central region and thereby forms a localized liquid-rich region on the substrate. As the substrate approaches close to the microwell array, the liquid of interest spontaneously fills the microwells without bubble formation based on the capillary interactions between the liquid and the surface of patterned PDMS and the

microchip. This sealing method was found to be highly reproducible in case of trials with water and PCR reagents, showing neither bubble-trap nor distinct interwell liquid volume variation. This technique can also be applied to the hydrophobic liquid case under the use of the reversely-patterned substrate and microchip.

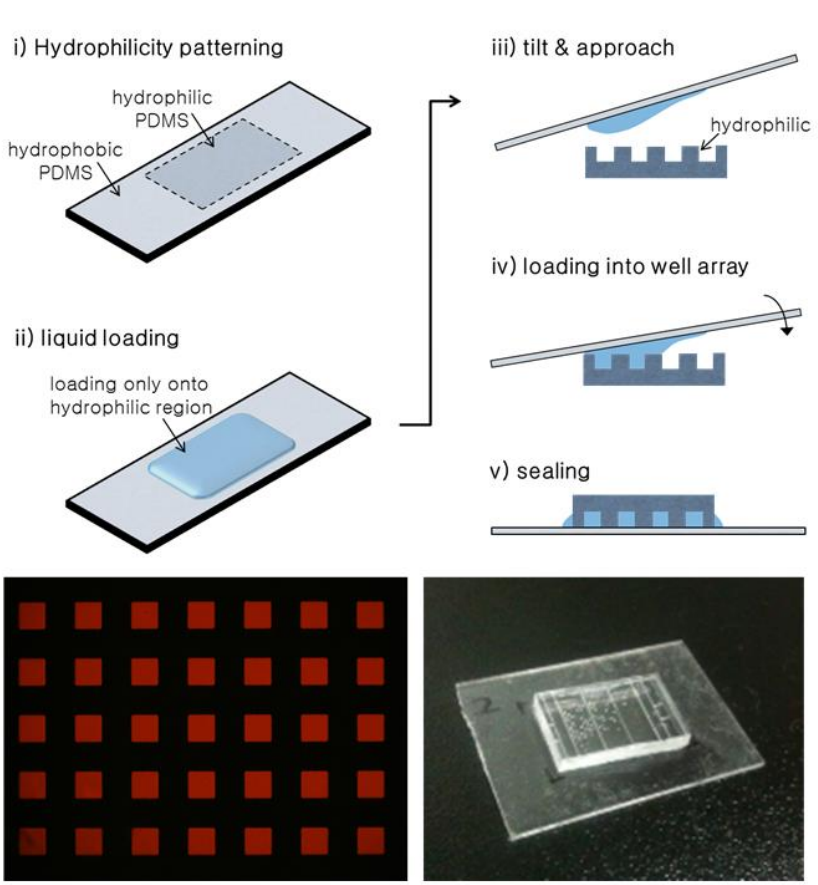

Figure 3.2 Bubble-free liquid loading into a microwell array. (A) method overview, (B) 500nM ROX (in water) loading result (C) an example of a sealed microwell array microchip

In order to achieve stable sealing and handling of the microchip, a custom-made microchip holder was also prepared (Figure 3.3). The microchip holder consists of two flat aluminum substrates having a window for microscope imaging. Four screw holes were provided to apply uniform pressure throughout the microchip. A heat transfer block made of brass was also prepared to deliver heat to the microchip enclosed by the assembled microchip holder.

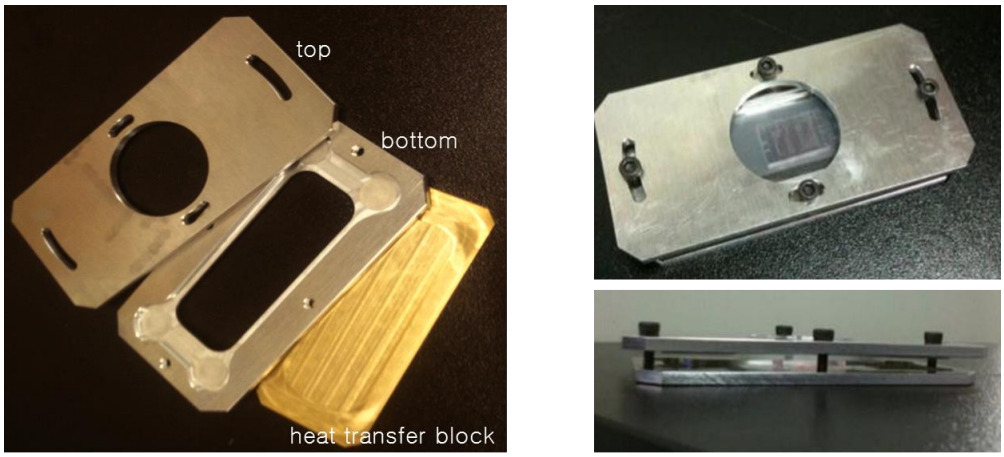

Figure 3.3 A custom-made microchip holder consisting of two flat substrates and a heat transfer block

3.1.4 Investigation of Microwell Isolation

After sealing of the microwell array, reaction chamber isolation test was performed (Figure 3.4). Firstly, microwells were filled with 500nM 5-carboxy-X-rhodamine (ROX, in water) and sealed. Drain channels were then replaced by 10mM

fluorescein (in water) through the drain channels. Spatial isolation of individual microwells was investigated by analyzing confocal microscope (TCS SP5 system, Leica Microsystems) images of microwells before and after thermocycling (50 cycles of 95˚C for 10s and 60˚C for 30s).

The fluorescein solution was confined only in the drain channel when it was firstly introduced. However, fluorescein molecules were found to be transported toward the microwells (up to ~200μm) along the PDMS-PDMS boundary after the thermocycling process. This result implies that interwell cross-contamination may occur during the thermocycling process; however, the fluorescein molecules did not reach microwells in this experiment. The fluorescein solution was also found to be completely dried after the thermocycling whereas the ROX solution was found to be confined very well within individual microwells. These results indicate that (i) there was no (or little) fluorescent dye transport between the microwells and the drain channel and (ii) each microwell was successfully sealed and isolated from its surroundings, thereby suppressing evaporation of water in it. Isolation of the microwells was also indirectly verified by confirming the strong bonding of the microwell array onto the PDMS substrate after the thermocycling.

On the other hand, a small amount of water (~11.5%) was found to be evaporated through gas-permeable PDMS at the nearest microwell around the drain channel; however, this loss is clearly not from the incomplete sealing of the

microchip. This water evaporation is expected to be minimized by (i) sealing the drain channel and (ii) placing a gas-impermeable film close to the microchip. Overall, the isolated microwells are expected to serve as small-volume reaction chambers for PCR applications free of cross-contamination.

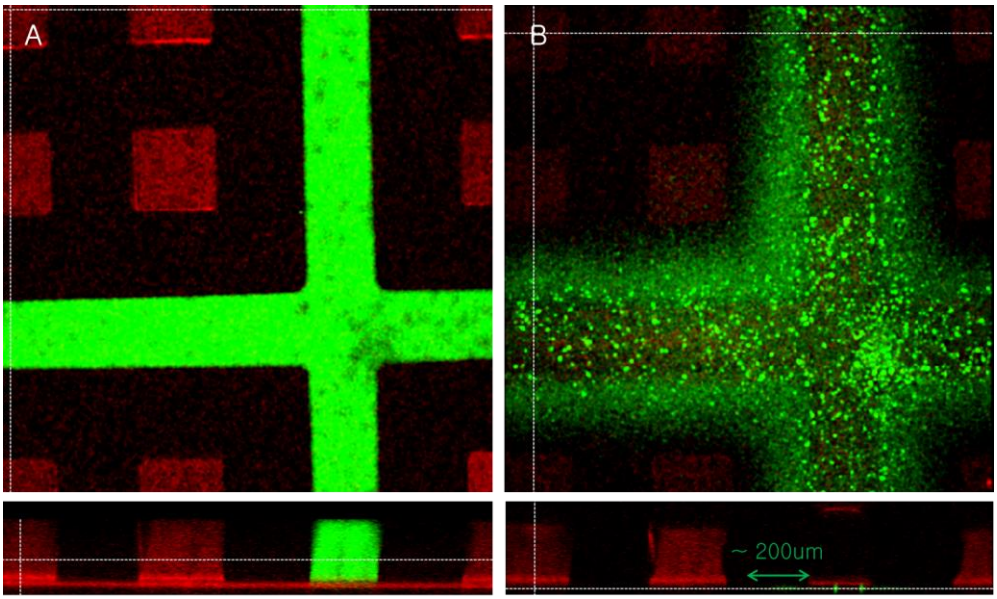

Figure 3.4 Confocal microscope images of a microwell array filled with two different fluorescent dyes. (A) before thermocycling; at the middle of the microchip, (B) after thermocycling; at the PDMS-PDMS boundary.

3.2 Experimental Setup and Data Analysis

Conventional real-time PCR systems employ a fluorescence detection unit along with a thermocycler. Most of the conventional equipments analyze PCR reactions taking place in microtiter plates or small-volume (less than ~100μL) tubes. In most cases, these equipments are not applicable to microchip analysis due to a lack of optical performance. In addition, non-flat surface of the conventional thermal blocks may inhibit uniform heat transfer throughout the microchip. High-throughput real-time PCR systems based on microfluidics and lab-on-a-chip technologies provide high-performance real-time PCR equipments with microchip applicability; however, these systems only allow their own specialized microchips to be analyzed. Therefore, a real-time on-chip PCR system compatible with the proposed microwell array is needed to be developed. This section describes the detailed information on the home-made real-time on-chip PCR equipment. Development of data analysis software is also described.

3.2.1 Real-Time On-Chip PCR System

To perform reliable thermocycling on a microchip, a thermocycler with a flat thermal block is required in order to provide stable and uniform temperature distribution throughout the microchip in each stage of a temperature cycle. There are a few commercially available thermocyclers providing a flat thermal block for the

purpose of supporting *in situ* PCR option. Among those flat-type thermocyclers AmpliSpeed thermocycler machine (Beckman Coulter) was chosen to be integrated to the real-time on-chip PCR system. The AmpliSpeed is the smallest and the lightest flat-type thermocycler commercially available and therefore makes system integration easy.

To read out fluorescence signals from multiple microwells in a microchip, a fluorescence detection unit should be equipped onto the thermocycle. For this, an upright-type light illuminator unit (BX-URA2, Olympus) equipped with two fluorescence filter units (U-MWIBA3 and U-MWIGA3 for green and red fluorescence signal detection, respectively) and a 75W xenon lamp (U-LH75XEAPO) was placed onto the thermocycler. Fluorescence images were acquired by using a CCD camera (DP72, Olympus) under the synchronized illumination of fluorescence excitation light, which was controlled by home-made filter unit changer and optical shutter, enabling automated two-channel fluorescence imaging. All functions described above were controlled and synchronized using LabView (National Instruments) interface in order to serve as a real-time on-chip PCR system. To maximize the number of microwells analyzed within a single optical field-of-view in a given optical system, a low-magnification objective lens (4x, UPLFLN 4x) was used in combination with a projection lens with a magnification of ~ 0.5, which fully utilizes the area of the 2/3'' CCD image sensor.

This configuration allows the analysis of 63 microwells within a single optical field-of-view. A motorized XY stage covering a whole microchip area may also be employed, increasing the total analysis throughput of the system. The whole system is shown in Figure 3.5.

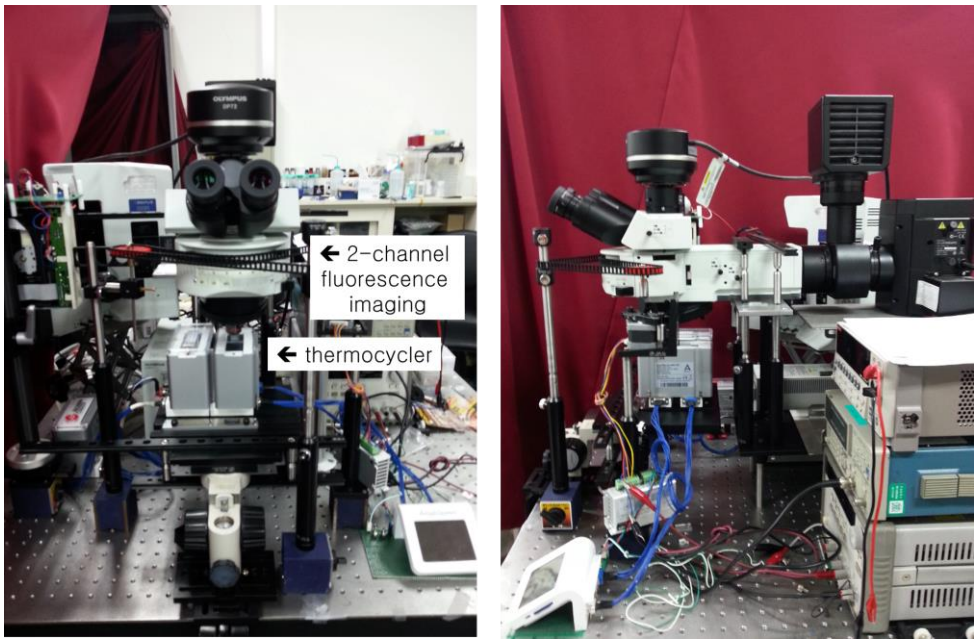

Figure 3.5 Real-time on-chip PCR system. Thermocycling and two-channel fluorescence imaging were synchronized in order to obtain fluorescence images of microwells during PCR.

3.2.2 Data Analysis

Data analysis was performed using a custom script written in MATLAB (MathWorks). Firstly, position of each microwell was determined from the red channel (normalization channel) image obtained before the thermocycling (Figure 3.6). A series of fluorescence intensities from a single microwell was then extracted from the sequential images obtained during the thermocycling. A representative signal value for each single microwell was defined as

$$W(\%) = \frac{I_G - I_{G0}}{I_R - I_{R0}} \times 100 \tag{3.1}$$

where I_G and I_R are the spatially-averaged green and red fluorescence intensities within a single microwell and I_{G0} and I_{R0} are those near the microwells serving as a background noise level for each detection channel. Here the red channel signal is used as a signal normalization factor because the red channel dye (ROX) is a PCR-independent fluorescent dye whereas the green channel fluorescence shows the amount of DNA molecules in the microwells. Finally, real-time amplification curves for individual microwells are generated by showing W values versus the number of PCR cycles (Figure 3.7). Based on the real-time amplification curves, subsequent analyses such as RNA quantification were carried out according to conventional quantitative PCR methods.

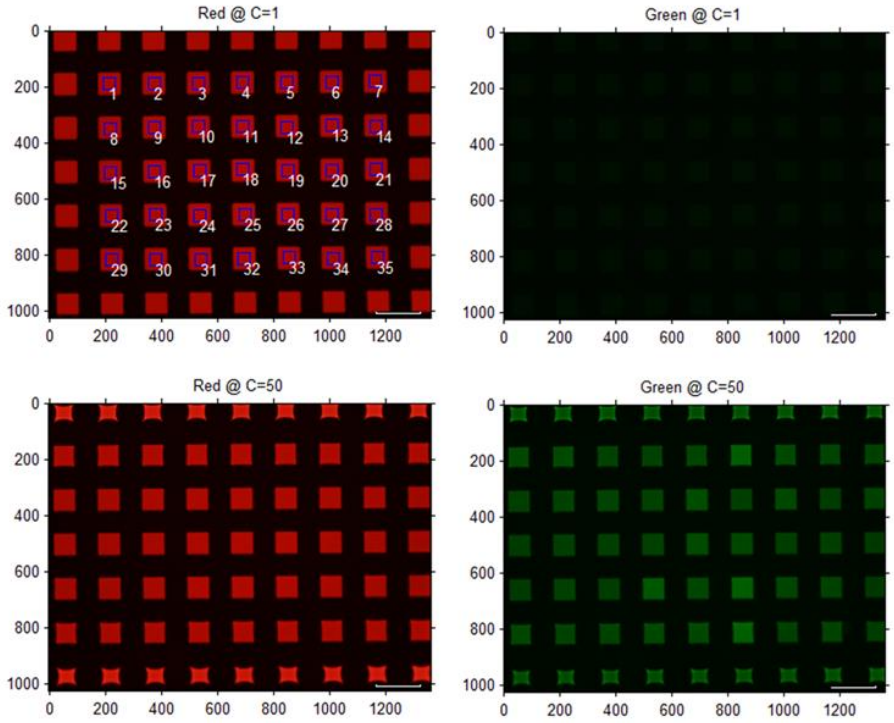

Figure 3.6. Data analysis software. Two-channel fluorescence images from the PCR cycle of ~1 and ~50 are shown.

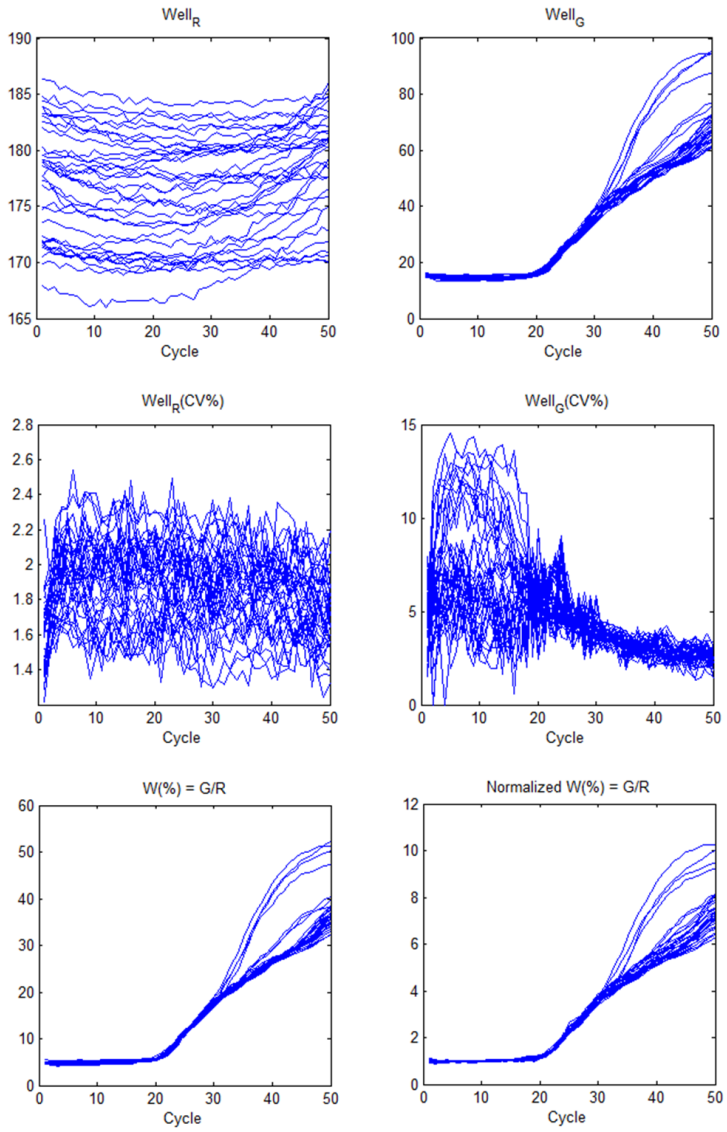

Figure 3.7. A representative data analysis result. *Mean*, *CV* and *W* values of the individual microwells are analyzed and shown.

3.3 PCR in small scale

Using the microwell array and the developed PCR system, small volume on-chip PCR experiment was performed. This section discusses challenges to be considered for small volume PCR such as influence of surface on PCR reaction. After scaling down a model PCR reaction from conventional to small volume environment, the constructed PCR system was validated in terms of accuracy, sensitivity and reproducibility of PCR result.

3.3.1 Model PCR Selection

Before performing small volume on-chip PCR experiment, a model PCR reaction was set up. By using conventional (~20μL volume) PCR, detection of glyceraldehyde 3-phosphate dehydrogenase (GAPDH) gene sequence from purified human genomic DNA was performed. GAPDH gene is a housekeeping gene which is stably expressed at high level in most cells and therefore usually considered as a control gene for RT-PCR. The primer sequence was designed as 5'- CAT CAC CAT CTT CCA GGA GC -3' (forward) and 5'- ATG CCA GTG AGC TTC CCG TC -3' (reverse), and the target amplicon length was ~ 474bp. By investigating various PCR conditions, successful DNA amplification conditions were found (Figure 3.8). After optimization a model PCR condition for on-chip PCR verification was determined as follows: primer concentration ~100nM and amount of target DNA ~20ng,

Thermocycling condition was also determined as follows: 3 min at 95℃, followed by 40 cycles of 10s at 95℃, 10s at 55℃ and 20s at 72 ℃. For quantitative PCR reactions, SYBR green I — a widely-used DNA intercalating dye — was additionally employed to detect DNA molecules and estimate the quantity of DNA.

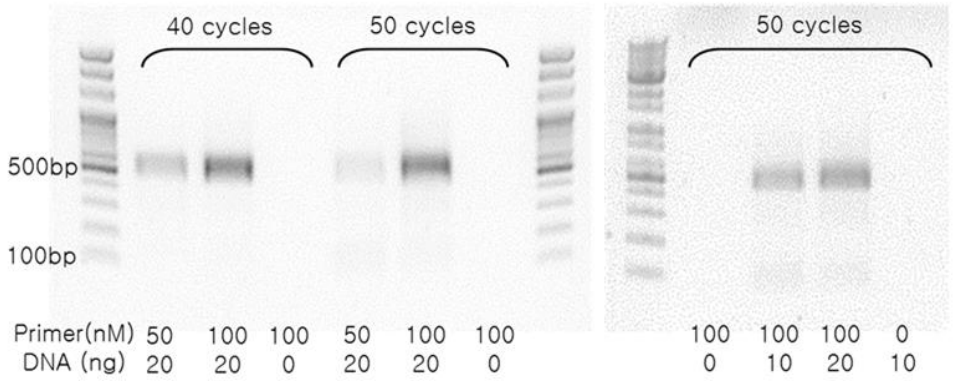

Figure 3.8 Conventional model PCR reaction result

3.3.2 Small Volume Considerations

In most cases of experiments in microfluidic environments, influence of reaction chamber surface becomes critical and therefore should be considered. The influence of surface is increased because of the increased surface-to-volume ratio; in this research, the surface-to-volume ratio of a microwell (volume ~10nL) is 2.78×10^4 m^{-1} whereas that of conventional PCR reaction volume (~20μL) is 2.21×10^3 m^{-1}

under the assumption of cube shape. The influence of the surface is, therefore, greater than tenfold in the microwell cases. In particular, PDMS surface has been reported to have an influence on PCR reactions, requiring extra cares to address it.

The large surface-to-volume ratio may inhibit PCR reaction through the surface adsorption of biochemical molecules such as enzymes, DNAs and dyes. Indeed, the model PCR reactions performed at first in the microwells were found to show no DNA amplification. To decrease the influence of PDMS surface on PCR reaction, several passivation molecules were tested. In particular, tween 20 and bovine serum albumin (BSA) were added in the PCR reaction mixture to achieve dynamic surface coating during the PCR reaction, i.e. the passivation molecules competitively participate in the surface interactions, rendering the PDMS surface free of non-specific adsorption of functional molecules. By virtue of the use of dynamic surface passivation approach, the model PCR reaction was successfully reproduced in the small-volume microwells (Figure 3.9).

Figure 3.10 shows representative fluorescence images obtained from successful on-chip PCR experiment. After thermocycling distinct fluorescence signal increase in green channel was detected. The ratio of W values before and after the thermocycling was obtained to be ~11.08. In case of microwells being located near drain channels, distinct shrinkage of microwells and corresponding increase of fluorescence intensities were found. This result shows the influence level of water

evaporation through PDMS in the microchip; however, most of the microwells which are not adjacent to the drain channels showed much less evaporation. By changing the number and arrangement of the drain channels, the influence of evaporation on the microchip can be much reduced. In addition, the influence of evaporation can be compensated thanks to the normalization channel (red channel) detection, yielding the compensated *W* values regardless of changes in the microwell volumes.

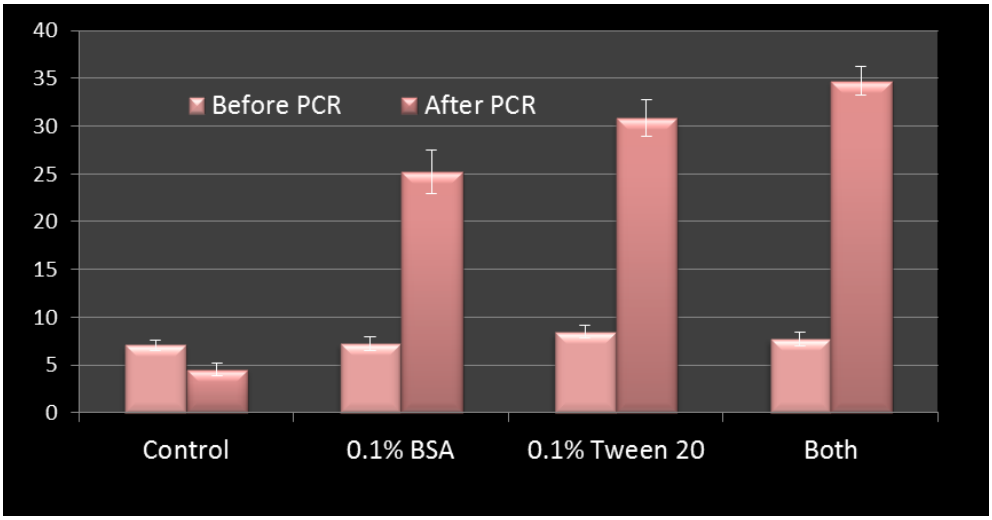

Figure 3.9 Dynamic surface passivation for small volume on-chip PCR. A model PCR reaction is not reproduced in a PDMS microwell array without passivation molecules. By adding passivation molecules in the reaction mixture, the model PCR reaction was successfully reproduced.

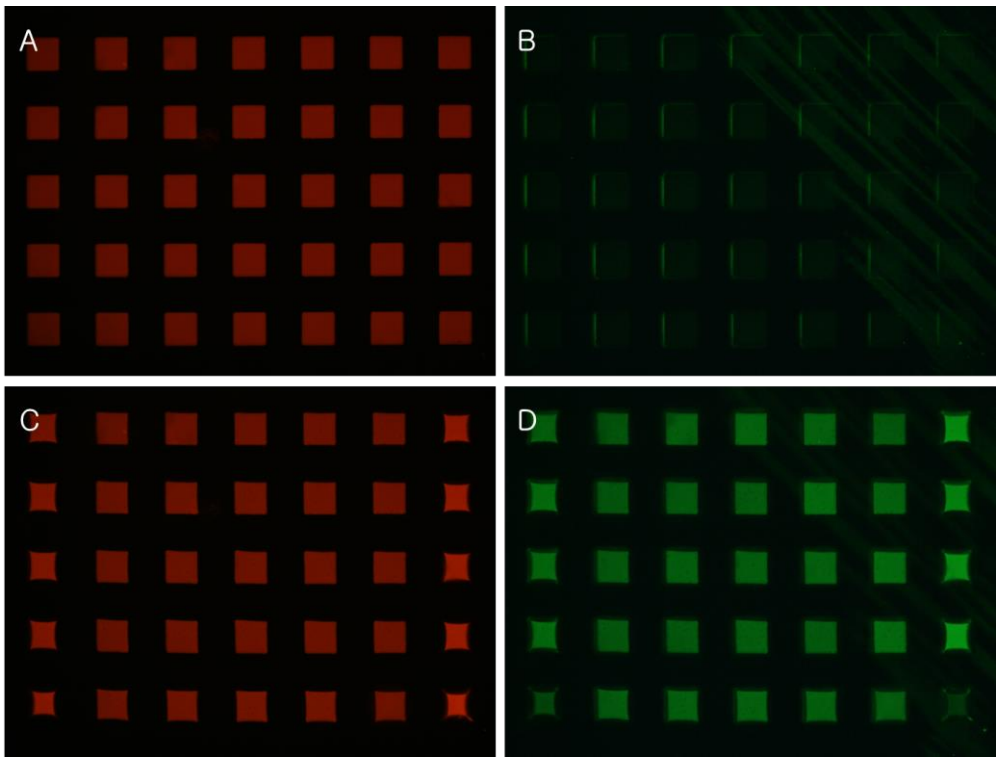

Figure 3.10 Representative fluorescence images obtained from on-chip PCR experiments. (A and B) Fluorescence images obtained from red and green channel before thermocycling. (C and D) Fluorescence images obtained from red and green channel after thermocycling. Distinct signal increases in green channel are observed. Microwell shrinkage is also observed in the microwells at the left and right side of the images. These microwells are close to the drain channels (not shown in the images) and therefore get shrunk due to water evaporation through PDMS.

3.3.3 On-Chip PCR Validation

Validation of the achieved small volume on-chip PCR was performed in various PCR conditions. As expected, PCR reaction mixtures containing human genomic DNA only showed the amplification of DNAs in the microwells whereas there was no distinct signal change in the conditions without DNA target or primers (Figure 3.11). In the case of DNA target, coefficient of variation (CV) of *W* values after the the thermocycling was found to be less than ~10%, showing good reaction reproducibility.

Finally, to prove that the increased fluorescence intensity in microwells reflects the amplification of target DNA sequence, the reaction product of on-chip PCR was collected and investigated (Figure 3.12). For this the PCR product was obtained from a microchip performing multiple identical PCR reactions and analyzed by gel electrophoresis. The collected on-chip PCR product was found to have the same length (~500bp) as the reaction product obtained from conventional tube-based PCR. The on-chip PCR product was further analyzed by Sanger DNA sequencing method. The sequence of on-chip PCR product was found to be matched with the target amplicon sequence, proving the successful reproduction of the model PCR reactions in microwell environments.

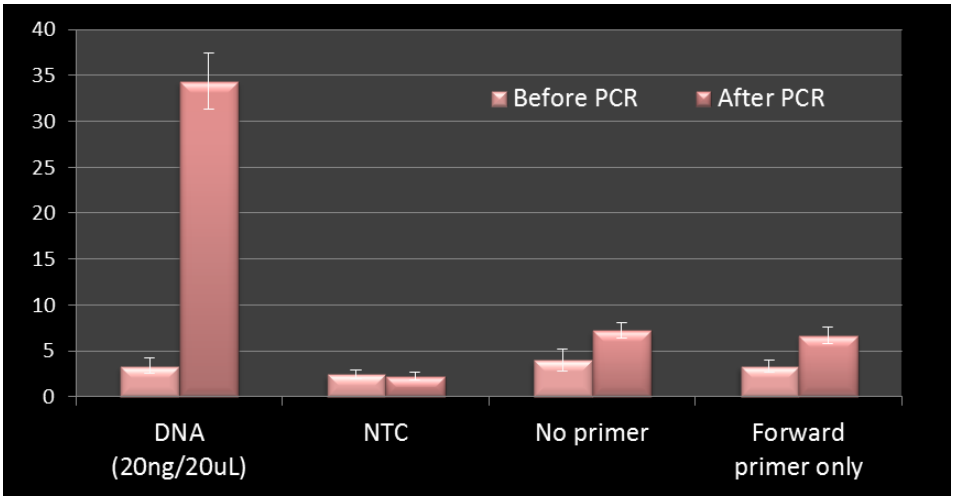

Figure 3.11 Small volume on-chip PCR results with various sample conditions. (from left to right) DNA target, no target control, no primer and forward primer only.

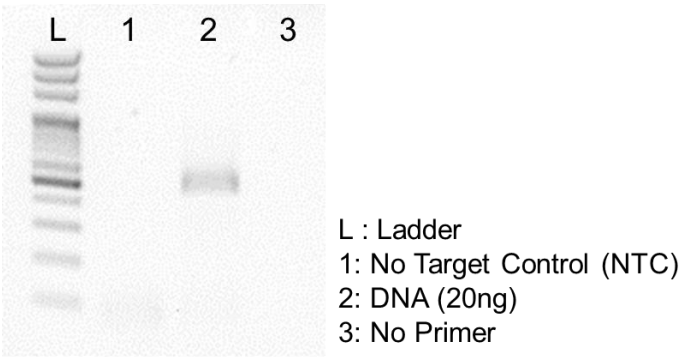

Figure 3.12 On-chip PCR product validation. The PCR product was collected from a microchip after the microchip detachment. PCR reaction with DNA target only results in the DNA amplification.

Chapter 4

‘One-Pot’ Lysis-RT-PCR

The use of microwell array has a potential to provide a large number of parallel RT-PCR reactions in high throughput, whereas its simple structure does not allow multi-step reactions with different reagents. Since there is no commercially-available single-step reagent providing cell-lysis, reverse transcription and DNA amplification in a fixed reaction volume, ‘one-pot’ lysis-RT-PCR condition should be developed in order to achieve single-cell RT-PCR in microwell environment. This chapter deals with challenges and solutions in determination of cell-lysis condition compatible with the subsequent RT-PCR process.

4.1 Considerations for True 'One-Pot' Lysis-RT-PCR

Currently, numbers of reagents for simplified, single-step RT-PCR are commercially available. Most of the reagents allow reverse transcription and subsequent DNA amplification in a single reaction chamber by employing 'hot-start' DNA polymerases which are activated by high-temperature incubation trigger introduced after the reverse transcription. Those 'one-step' RT-PCR reagents mostly require preparation of purified RNA as a template for the reaction, inhibiting introduction of intact cell samples into the reagent mixture. Some purification-free RT-PCR reagents (ex. CellsDirect One-Step qRT-PCR Kit, Invitrogen) provide specially-designed cell-lysis buffer and enable utilization of cell lysate as template in RT-PCR. Although the purification-free cell-lysis buffer simplifies RT-PCR process in terms of sample preparation, sequential addition of reagents is required in order to retain buffer compatibilities. In addition, cell-lysis process usually accompanies relatively high temperature (~75˚C) incubation which may affect the activity of reverse transcriptase during the cell-lysis step. In short, there has not been any reliable single-chamber RT-PCR method requiring no extra cares such as sequential reagent addition or pre-incubation at high temperature.

To perform single-cell RT-PCR in microwell environment, true 'one-pot' lysis-RT-PCR including cell lysis, reverse transcription and DNA amplification should be developed. To be more specific, mild cell-lysis condition in that activity of reverse

transcriptase is conserved should be found. The determined buffer condition should also retain enzyme activities as well as RNA integrity. To satisfy these requirements, various reagent conditions for the compatible use of intact cell template have been tested.

4.2 Determination of Cell-Lysis Condition

To make intracellular RNA molecules accessible to the RT-PCR reagents, cells should be lysed (or dead) through the destruction of cell membrane. To determine whether cells are alive or dead in the controlled cellular environment, a cell-viability test reagent (LIVE/DEAD Viability/Cytotoxicity kit for mammalian cells, Molecular Probes), which indicates cell fate by showing different fluorescence signals, is used. Since the cell-viability test reagent is considered to be used at room temperature only, the availability of the reagent under high-temperature conditions was firstly tested in order to prevent false-positive cell-lysis determination. Based on the functional inspection of the cell-viability test reagent under various thermal incubation conditions, the functionality of the reagent was proven to be still maintained after incubation at 60˚C for 40 min (Figure 4.1). In addition, the cell-viability test reagent was found to show no fluorescence signals after high-temperature incubation (90˚C, 30 min). Next, live cells were incubated with the cell-viability test reagent using conventional incubation protocol (room temperature, 30 min) to make cells show strong intracellular ‘live (green)’ fluorescence signals. Cell-lysis can then be confirmed based on (i) the spreading of intracellular green fluorescence signals throughout the extracellular environment and (ii) arising of ‘dead (red)’ fluorescence signals within the cells, both of which directly and indirectly indicate the destruction of cell membrane, respectively. Various thermal and/or chemical cell-lysis conditions were tested based on this approach.

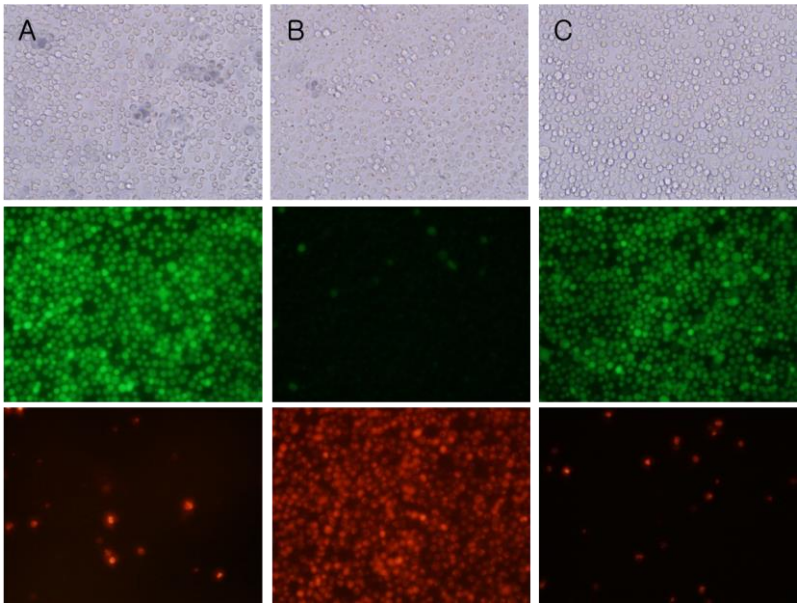

Figure 4.1 An availability test of the cell viability test reagent after high-temperature incubation. Images are taken after 30 min incubation of (A) live cells with normal reagent, (B) dead cells with normal reagent, and (C) live cells with heat-treated (60˚C, 40min) reagent. Experiment (A) and (B) were conducted as control experiments. A 96-well plate placed onto a hot plate was used for cell incubation.

4.2.1 Thermal Lysis

To inspect the effect of thermal incubation on the cell viability, cells were incubated at three different temperature conditions — 23˚C, 50˚C and 90˚C. In this experiment, HL-60 cell line (human promyelocytic leukemia cells) was used as a model cancer cell line. Deionized water was firstly chosen as a thermal-lysis buffer because most of all RT-PCR reagents are mainly composed of water. The use of deionized water

may also help cell-lysis process due to the mismatch of intra/extra osmotic pressure. Most of the cells were found to be dead after incubation at 90˚C for 25 min whereas there was no distinct change in cell viabilities in the room temperature incubation condition (Figure 4.2). In case of relatively mild temperature condition (~50˚C), partial cell death was observed; however, the majority of cells were found to be alive. The same experiment result was obtained from the microwell environment (Figure 4.3).

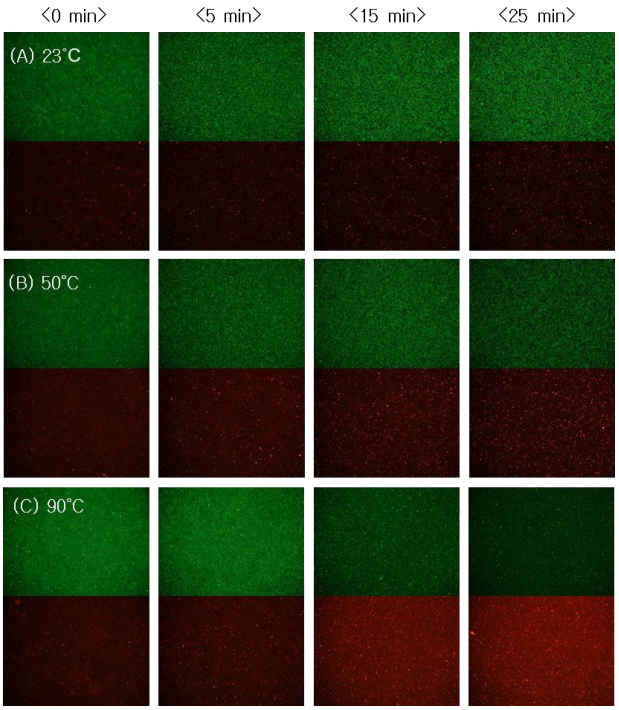

Figure 4.2 Time-lapse images of cell viability signals in three different incubation conditions. Deionized water was used as an extracellular buffer in this experiment.

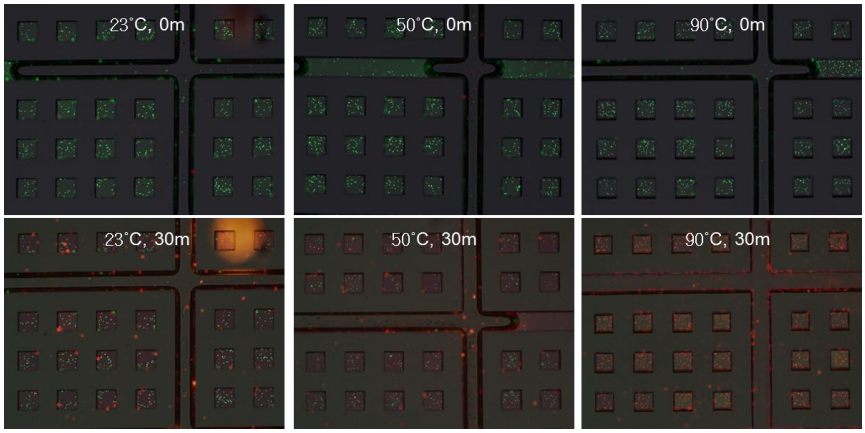

Figure 4.3 Cell viability test in microwell environments under three different thermal incubation conditions. Images were merged from two fluorescence images and a bright-field image.

4.2.2 Chemical Lysis

To make cell-lysis step compatible to subsequent reverse transcription process, high-temperature cell-lysis condition should be avoided. In this context, the use of detergents having cell-lysis capability can mitigate the requirements of thermal incubation. Among various kinds of detergents two widely-used cell-lysis detergents - Tween 20 and Nonidet-P40 (NP-40) - were tested. These mild detergents are only capable of destroying cell membranes without nucleus lysis. Therefore, extraction of genomic DNA is suppressed, potentially facilitating gene expression profiling or whole transcriptome analysis with low sample noise.

To suppress the effect of convection within an incubation chamber, a drop of 2% detergent solution was added into detergent-free incubation chambers to make the final detergent concentration of ~0.1% while cells are incubated. In all temperature conditions studied, both detergents (tween 20 and NP-40) were found to increase efficiency of cell-lysis compared to that of deionized water. Especially, cells were found to be completely lysed after 25min incubation at room temperature, showing the availability of room-temperature cell-lysis process (Figure 4.4). In this experiment, the influence of detergent on cell-lysis is only studied. The influence of detergents on RT-PCR reaction is discussed in the next section.

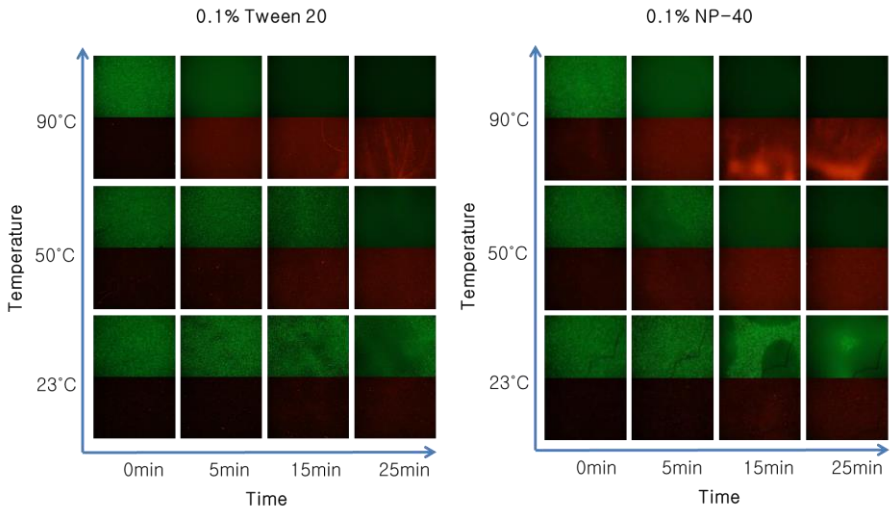

Figure 4.4 Cell lysis with the help of detergents. In all temperature conditions, cell lysis was completely finished within 25 min for both detergents.

4.2.3 Thermostable Reverse Transcriptase

To make the cell-lysis step compatible to subsequent reverse transcription process in single-step, fixed volume lysis-RT-PCR, reverse transcriptase must maintain its enzymatic activity during the cell-lysis process. Another approach other than the use of mild cell-lysis condition is to use a thermostable reverse transcriptase which endure relatively high temperature (usually up to ~70˚C). In this research, both approaches were carried out in parallel in order to meet the requirements for the 'one-pot' lysis-RT-PCR process.

4.3 'One-Pot' Lysis-RT-PCR Using Cell Samples

Although mild cell-lysis conditions were determined, there are more issues to be addressed for direct 'one-pot' lysis-RT-PCR using cell samples. Cells are expected to provide RNA molecules to be amplified and detected through RT-PCR reactions; however, they may also cause some negative effects on RT-PCR reactions when they are directly introduced to the reaction environments. For instance, intracellular ribonuclease (RNase) may be released into the reaction mixture and cause degradation of RNA molecules. Besides, some other potentially active intracellular materials may have a harmful effect on the desired reaction. Cell lysate itself may also inhibit RT-PCR reactions because of its chemical interactions with RT-PCR-related biochemical molecules. Indeed, simple addition of cell sample into the pre-designed RT-PCR conditions gave no amplification result, requiring sample-specific handlings. An optimized reagent condition in that cellular RNA molecules are well conserved and inhibitory factors are successfully suppressed should be determined for reliable lysis-RT-PCR reactions from cell samples.

4.3.1 Ribonuclease Inhibitors

In addition to using RNase-free labware including tools and reagents, the use of RNase inhibitors was considered for the purpose of protecting cellular RNA released during cell-lysis. In this work two different RNase inhibitors — RNase Inhitibor (RI,

Invitrogen) and SUPERase-In RNase Inhibitor (SUPERase-In, Invitrogen) — have been tested in order to protect RNA molecules in the reaction environments [61-63]. RI is a general-purpose potent inhibitor of neutral pancreatic RNases such as RNases A, B, and C and SUPERase-In is a non-human origin RNase inhibitor which is especially expected to inhibit troublesome RNases including RNase 1 and T1.

Before performing direct lysis-RT-PCR experiments, the influence of the use of RNase inhibitors on conventional RT-PCR reactions was investigated. After optimization of RT-PCR conditions, a combinatorial use of RI and SUPERase-In was found to give no distinct negative effects on the conventional RT-PCR reactions (Figure 4.5). The modified RT-PCR conditions with the addition of RNase inhibitors were further tested whether they provide the same experimental result in the existence of cell lysate. For this experiment, cells with controlled cell numbers were firstly incubated in deionized water with 0.5% NP-40 at 70˚C for 10 min to serve as a cell lysate without active biochemical functionalities, only containing chemical composition of cells. The prepared cell lysate was then added in the modified reagent conditions (with RNA target included) for RT-PCR reaction. In all cell lysate concentrations studied, RT-PCR reaction was found to be successfully reproduced (Figure 4.6). Especially, the experimental condition with the addition of ~ 1000 cells in 20μL, which is equivalent to ~ 0.5cell/10nL or 0.5 cell in the volume of a single microwell, gave a distinct amplification result with only a little decrease in the

amplification, suggesting the feasibility of inhibition-free single cell RT-PCR in the designed microwells.

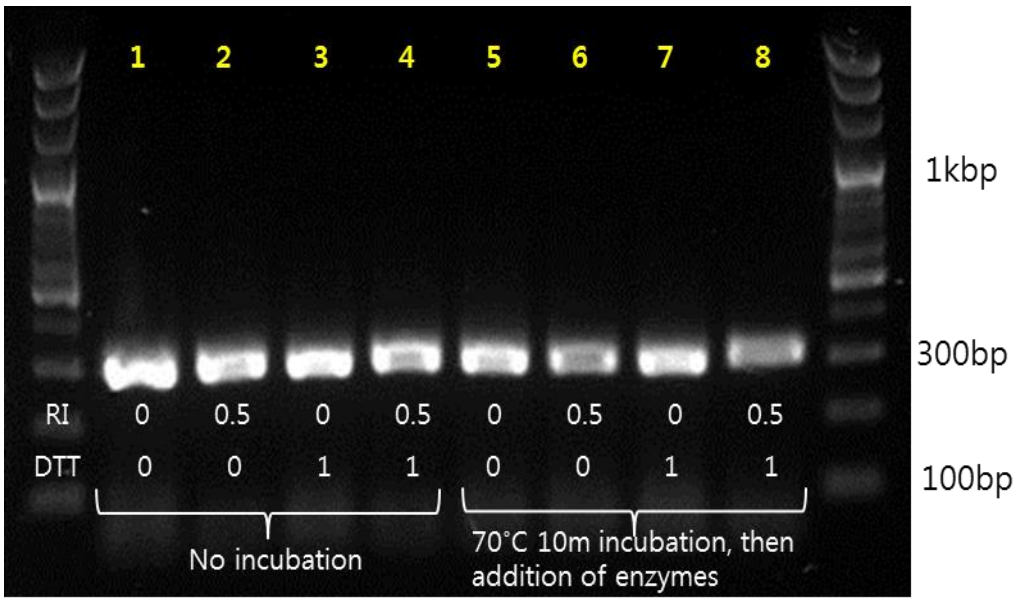

Figure 4.5 Investigation of the influence of the use of RNase inhibitors on conventional RT-PCR conditions. (1~4) All reagents were mixed before RT-PCR. (5~8) The reagents without enzymes (reverse transcriptase and DNA polymerases) were firstly mixed and incubated at 70˚C for 10 min before the addition of the enzymes followed by RT-PCR. SUPERase-In was added in all (1~8) conditions since it guarantees the compatibility with RT-PCR. DTT was added because RI requires it for its activity.

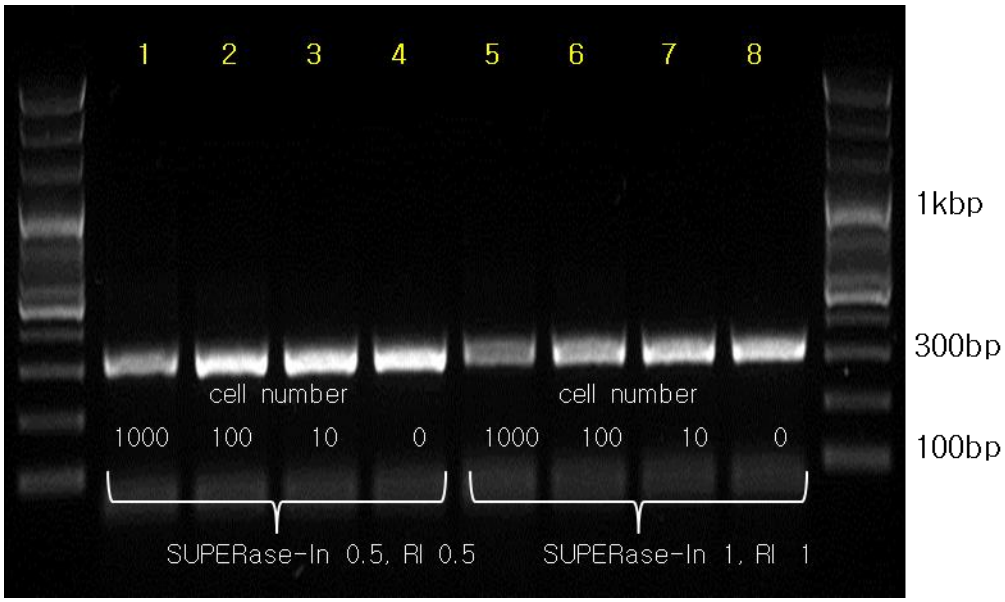

Figure 4.6 Investigation of the influence of the cell lysate on RNA-containing RT-PCR conditions. To prepare cell lysate without biochemical functionalities, cells with controlled cell numbers were incubated in deionized water with 0.5% NP-40 at 70˚C for 10 min before they were added into the RT-PCR reagents. The number of added cells are ~1000 (1, 5), ~100 (2, 6) and ~10 (3, 7). No cell lysate was added in the conditions 4 and 8. Experimental investigation was conducted in two different RNase inhibitor concentrations as noted in the figure. A little reaction inhibition was found in the conditions with the addition of ~1000 cells (1, 5), in which the concentration of cell lysate is comparable to that of microwell RT-PCR in this work.

4.3.2 Direct Lysis-RT-PCR from Cells

After obtaining successful RT-PCR result from the reagent conditions containing RNase inhibitors and cell lysate, lysis-RT-PCR conditions targeting cellular RNA were investigated. As the first step of the experiments, cell lysate was prepared by suspending cells in 0.1% NP-40 (in water) containing 1mM DTT and RNase inhibitors with various concentrations. Here the RNase inhibitors were added to conserve cellular RNA released during the cell lysis step. The cell lysate was then incubated at 70˚C for 90s to ensure complete cell lysis before it was added to RT-PCR reagent as an amplification target. After a series of experimental investigations, successful cellular RNA amplification was observed in some RT-PCR conditions containing a sufficient amount of RNase inhibitors regardless of the amount of cells (Figure 4.7). In contrast, blurred amplification bands were observed in the conditions with a relatively small amount of RNase inhibitors. Besides, in the conditions with both high cell concentrations and low RNAse inhibitor concentrations, no amplification was observed maybe due to the lack of RNA-preserving capability of those conditions. All those results show that RNase inhibitors truly prevent the degradation cellular RNA by inhibiting activity of RNAse released from cells.

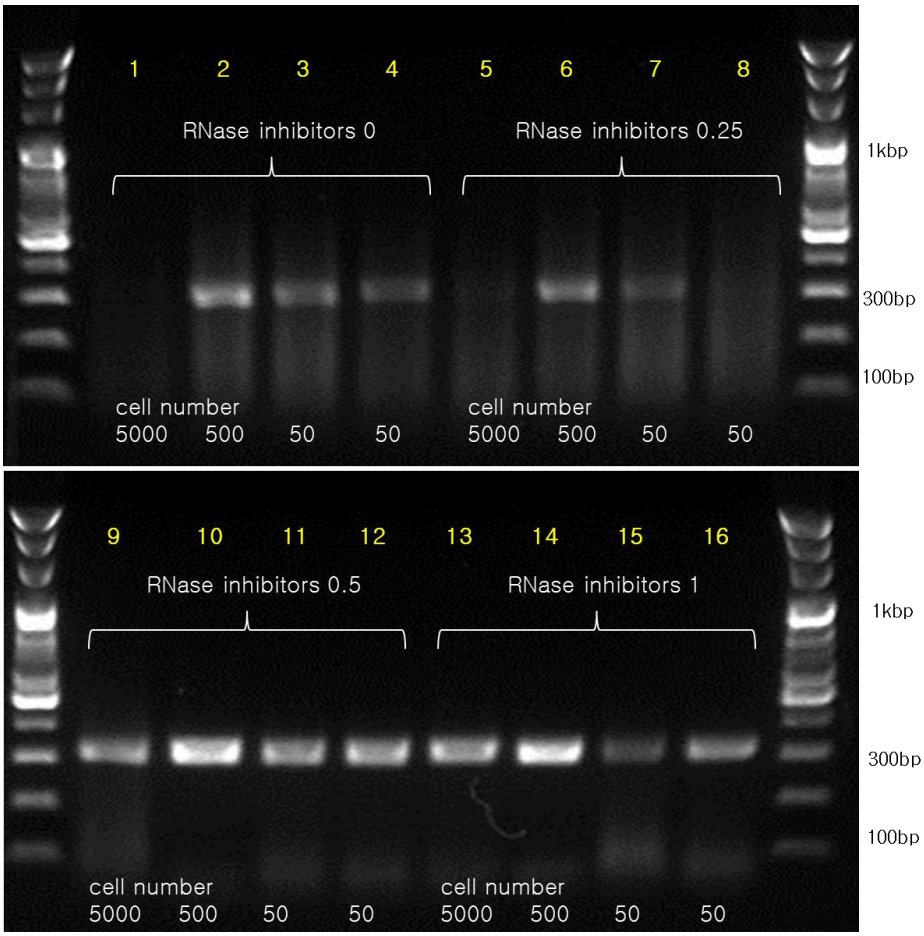

Figure 4.7 RT-PCR results of cellular RNA targets with various RNase inhibitor concentrations and cell numbers. Cell lysate was prepared by incubating cells in 0.1% NP-40 (in water) containing 1mM DTT and RNase inhibitors (RI and SUPERase-In) with various concentrations at 70˚C for 90s and then added into RT-PCR reagents.

To achieve a true ‘one-pot’ lysis-RT-PCR condition employing intact cell target, neither sequential additions of reagents nor thermal incubation steps inbetween them are allowed; i.e. a thermal incubation step is only allowed after all reagents including cells and enzymes are mixed. To find an optimal incubation condition that gives successful RT-PCR result, a series of low-temperature incubation conditions were investigated under the fixed reagent condition that works well with thermally-treated cell lysate. Surprisingly, all the low-temperature incubation conditions including room temperature incubation and on-ice incubation provided successful target amplifications (Figure 4.8). The establishment of true ‘one-pot’ lysis-RT-PCR conditions has a series of significant meanings as following:

(i) It simply employs intact cell samples as an amplification target, requiring no target preparation step such as RNA purification.

(ii) No pre-incubation step is required, guaranteeing stable biochemical activities of participant enzymes.

(iii) No sequential addition of reagent is needed, making the obtained condition applicable to single-volume RT-PCR approaches such as microwell technologies.

In combination with microwell-based small-volume on-chip PCR system, the ‘one-pot’ lysis-RT-PCR reagent condition is expected to serve as a promising platform for

single-cell gene expression profiling. Integration of small-volume on-chip PCR condition, ‘one-pot’ lysis-RT-PCR condition, microwell-based single-cell trapping and real-time analysis of RT-PCR reaction is discussed in the next chapter.

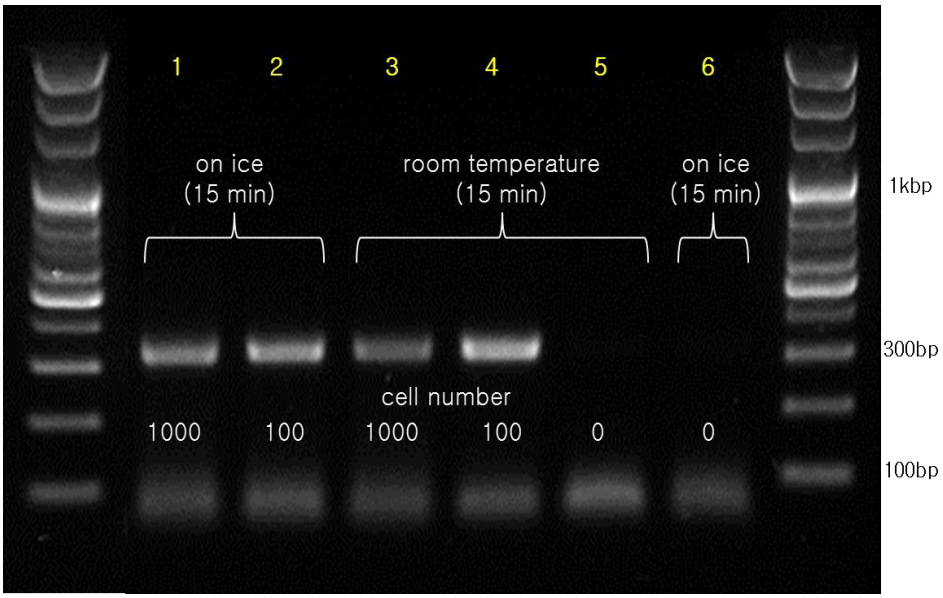

Figure 4.8 ‘One-pot’ lysis-RT-PCR using intact cells as amplification target. All the participant reagents including cell target and enzymes were firstly mixed and incubated at low temperatures for 15min. Samples only with cell addition clearly showed amplified product.

Table 4.1 ‘One-pot’ lysis-RT-PCR reagent condition

Reagent		Source conc.	Volume	Final conc.
PCR reaction mix	CellsDirect One-Step qRT-PCR Kits, Invitrogen	2x	10μL	1x
Primer (target gene : GAPDH, amplicon length ~ 312bp)	Forward: 5’-CCA TCT TCC AGG AGC GAG ATC-3’ Reverse: 5’- GGA CTG TGG TCA TGA GTC CT-3’	5μM	1μL / 1μL	250nM
Reverse transcriptase and DNA polymerase	CellsDirect One-Step qRT-PCR Kits, Invitrogen	50x	0.5μL	1.25x
RNase Inhibitor	Invitrogen	40U/μL	0.5μL	1U/μL
SUPERase Inhibitor	Invitrogen		0.5μL	
DTT	Invitrogen	20mM	1μL	1mM
NP-40	Invitrogen	10%	0.5μL	0.25%
Cell (in PBS)	HL-60	vary	1μL	vary
RNase-free water	Thermo Scientific		4μL	
Total		20μL		

4.3.3 Validation of 'One-Pot' Lysis-RT-PCR

In the experiments for 'one-pot' lysis-RT-PCR conditions, PCR primers with potential amplified products from both DNA and RNA were used. To confirm that the amplification product was indeed obtained not from DNA but from RNA of cells, RNA-specific quantitative RT-PCR analysis was designed and performed. For this a commercial RNA-specific RT-PCR assay targeting GAPDH gene (Hs99999905_m1, Taqman probe, Life Technologies) was employed. Figure 4.9 shows real-time amplification curves for various RT-PCR target conditions including DNA, RNA and cells. In case of DNA target conditions, the amplification curves showed only a small amount of signal increase after the cycle number of ~ 35, showing very similar shape with those of non-target-control (NTC) conditions. This result shows that the primer set does not give specific amplification product from DNA target. The late small signal increases in DNA target and NTC conditions may be from formation of primer dimers during PCR reactions. On the other hand, sample conditions with RNA target showed conventional RT-PCR amplification curves, proving RNA specificity of the selected primer set. In case of cell target conditions, amplification curves were very similar to those of RNA target conditions. Therefore, amplification of cellular RNA can be inferred from the real-time amplification curves fot the cell target conditions.

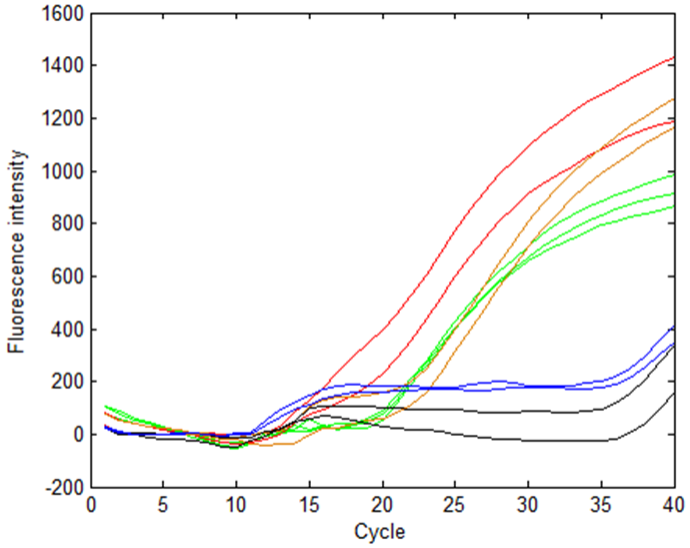

Figure 4.9 Real-time amplification curves from various RT-PCR target conditions. (red) 1000 cells, (orange) 100 cells, (green) RNA (blue) DNA, and (black) non-target-control. Real-time RT-PCR was performed by the 7500 Real-Time PCR System (Applied Biosystems).

Chapter 5

Single-Cell RT-qPCR

Cells provide RNA molecules to be amplified through RT-PCR reactions whereas at the same time their lysate inhibits PCR reactions at high cell concentrations. Single-cell RT-PCR reaction can only be achieved under relevant experimental conditions such as reliable confinement of single cells and cell lysate concentrations in microwells. In this chapter, single cell trapping and confinement assisted by a micromachined microwell array are demonstrated. This chapter also describes the integration of real-time small-volume on-chip PCR system and ‘one-pot’ lysis-RT-PCR conditions in order to achieve quantification of single-cell gene expressions.

5.1 Multivolume Microwell Array

In order for single cells to be analyzed independently, individual single cells should be loaded into different and spatially-isolated reaction chambers. Various approaches employing microfluidics and/or lab-on-a-chip technologies have been developed for single cell loading and subsequent single cell analysis in high throughput. In most cases, obtaining single-cell distribution usually relies on Poisson distribution, yielding single-cell samples out of lots of empty samples. To achieve Poisson distribution of single cells, one usually employs a number of reaction chambers with diluted cell samples. The use of diluted cell samples inevitably cuts down the fill factor and corresponding analysis throughput, which is one of the key advantages of parallelized single cell analysis.

Additionally, the volume of reaction chamber is usually adjusted to be comparable to the volume of single cells in order to successfully confine single cells in individual single reaction chambers and exclude the loading of two or more unwanted cells in them. The limited reaction volume range may be critical in some applications requiring high sample dilution factors.

To address both analysis throughput and reaction volume considerations for high-throughput single-cell RT-PCR, the use of a multivolume microwell array has been proposed and validated. By designing two microwell arrays having different volumes but the same spatial origin, the issues on analysis throughput and reaction

volume were successfully decoupled.

5.1.1 Strategy

A multivolume microwell array consists of two (or more) microwell arrays having different microwell volumes but identical spatial origins. The two microwell arrays are assembled into a single microwell array, and all the microwells consisting of the microwell array become paired after they are assembled since all individual microwells within each microwell array share their spatial origins (Figure 5.1). When this strategy is utilized for high-throughput single cell loading with high dilution factors, a microwell with small volume serves as the microwell for single cell confinement while the other microwell with large volume provides the desired reaction volume dilution factor.

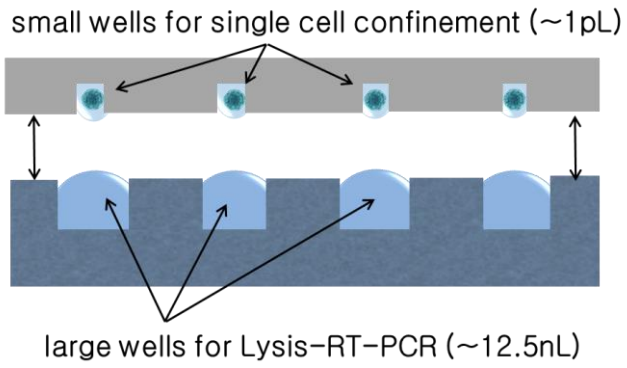

Figure 5.1 Multivolume microwell array strategy

5.1.2 Volume Considerations

Recently, inhibition of RT-PCR reaction by cell lysate was reported by White *et al*.; in their research, RT-PCR reaction was found to be significantly inhibited by cell lysate at concentrations in excess of ~0.2 cells/nL [52]. This research result suggests that single cells be contained in at least ~5nL reaction volume in order to serve as RT-PCR target for reliable amplification. Under the consideration of the volume of single cell (~ 1pL), loading of the diluted cell sample into a microwell array does not seem applicable to inhibition-free single cell RT-PCR since it requires extreme dilution accompanying severe reduction in the practical analysis throughput.

Based on the rule described above, a microwell with the final well-to-cell volume ratio of ~ 5000 is minimally required in order to provide a reliable gene amplification from single cell samples. The multivolume microwell array in this work, therefore, was designed to allow high-throughput single-cell confinement with high dilution factors (Figure 5.2). To be more specific, microwells for single cell trapping were designed to have the size range comparable to the size of single cells, and microwells for single cell dilution were designed to have a volume of ~12.5nL. Finally, the total well-to-cell volume ratio was obtained to be ~ 1.25×10^4, providing sufficient dilution of single cell lysate for single cell RT-PCR in microwell environments.

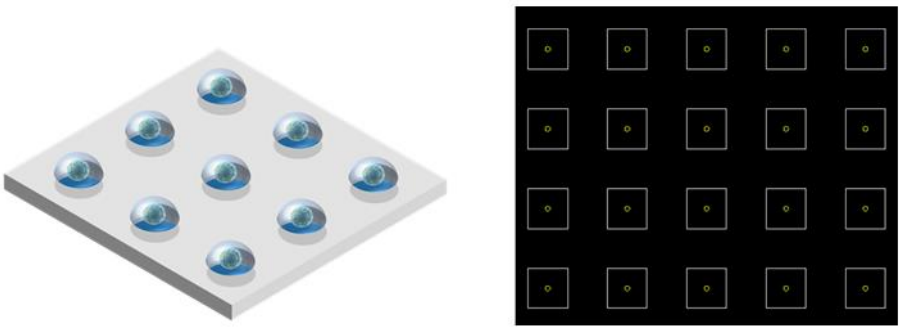

Figure 5.2 (left) A schematic diagram of a single cell array (right) Design of a multivolume microwell array. Small microwells (yellow) are for single cell trapping and large microwells (white) are for dilution of single cell lysate.

5.2 Single-Cell Loading and Isolation

Since the multivolume microwell approach employs two microwells with different volumes (or sizes), a distribution of microwells on a chip is mainly determined by the arrangement of larger microwells; as a result, smaller microwells inevitably have sparse distribution compared to their size. In this work, circular microwells with a diameter of 15 ~ 30μm were employed for single-cell trapping [64]. Those cell-trapping microwells, on the other hand, were positioned every 500μm on a chip due to the arrangement of the paired large wells for dilution of single cell lysate. Therefore, loading single cells into the cell-trapping microwells with excluding those cells from other part of the chip is therefore very important. In addition, transfer of the trapped single cells into the large microwells and corresponding isolation of individual reaction chambers should be achieved. The trapping and isolation of single cells using a multivolume microwell array were studied.

5.2.1 Experimental Preparation

For the preparation of cell samples, HL-60 cells were maintained by culturing using conventional cell culturing method. The cultured cell samples (originally contained in cell culture medium) were separated though density-gradient centrifugation method using a density-gradient medium (OptiPrep, Sigma Aldrich). After density-gradient centrifugation only viable cells were separated and collected as a final

product. The collected viable cells were then resuspended in phosphate buffered saline (PBS) solution with 20μg/mL bovine pancreatic ribonuclease A (Sigma Aldrich) at 37 ℃ for 1h to remove unwanted extracellular RNA molecules. After RNAse A treatment the cells were washed twice with PBS and resuspended in PBS with 20μg/mL ribonuclease A.

A PDMS microwell array with cell-trapping microwells was prepared through soft lithography. The surface of PDMS microwell array was then passivated by soaking the microwell array in PBS solution with 0.01% BSA for 12h. This BSA treatment was found to make cell washing easier after the cell loading.

5.2.2 Single Cell Trapping

Various single cell loading techniques have been developed and they include the use of microfluidic channels and/or microwells. Among those various cell-loading approaches a simple gravity-driven cell-loading method was employed in this work (Figure 5.3). Firstly, the concentration of cells was adjusted to be ~ 1×10^6 cells/mL based on the cell counts measured by a cytometer microchip (C-chip, NanoEnTek). The cell suspension was then added onto a microwell array already soaked in PBS solution with 20μg/mL ribonuclease A. After allowing 30min settling of cells the microwell array was washed more than ten times with PBS in order to remove

untrapped cells. The washing step results in a microwell array with trapped cells which is now ready for the microwell assembly step.

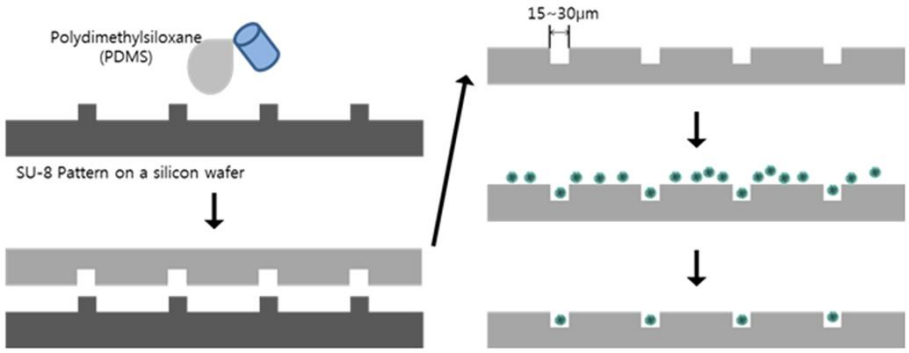

Figure 5.3 A schematic view of preparation of a cell-trapping microwell array and the gravity-driven single cell trapping and washing using the microwell array.

To investigate the throughput and efficiency of single cell trapping, a microwell array with a dense microwell distribution was used. Based on the size distribution of HL-60 cells, microwells with four different microwell sizes (15μm, 20μm, 25μm and 30μm) were prepared and investigated (Figure 5.4). The height of microwells was determined as ~20μm. After washing step single cell trapping was found to be achieved in ~40% of microwells with a diameter of 15 μm while most of the other wells were found to be empty (Figure 5.5). PDMS microwell array with cell-trapping microwells was prepared through soft lithography. The surface of PDMS

microwell array was then passivated by soaking the microwell array in PBS solution with 0.01% BSA for 12h. This BSA treatment was found to make cell washing easier after the cell loading.

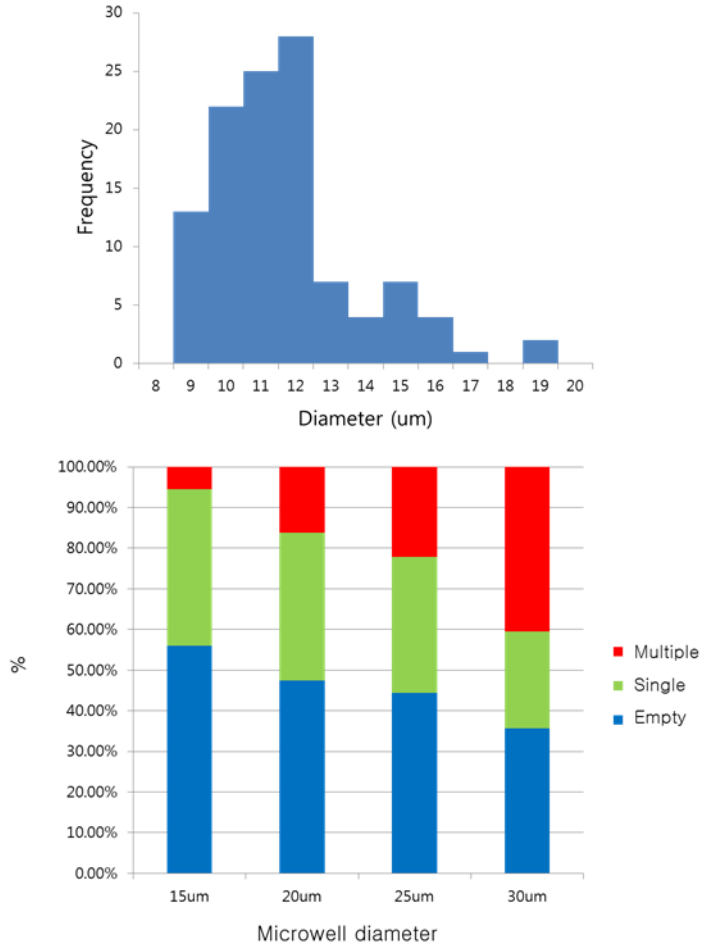

Figure 5.4 (top) Size distribution of HL-60 cells obtained by microscope imaging. (bottom) Cell occupancies investigated under various microwell sizes.

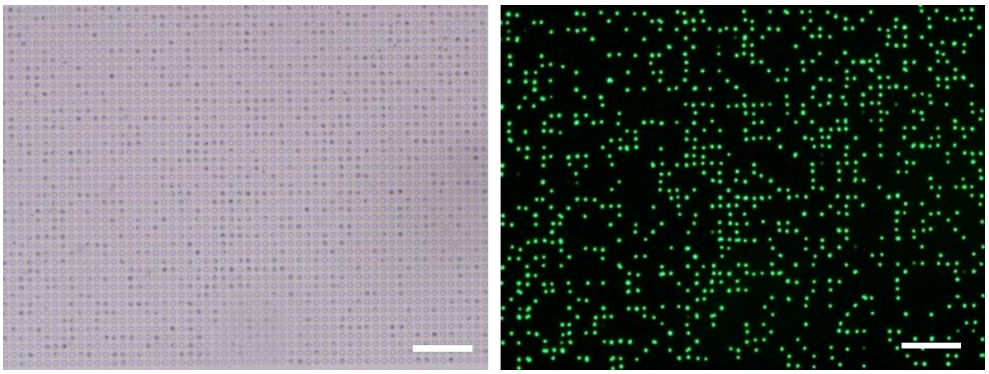

Figure 5.5 A microwell array with trapped single cells. Cells were stained with a cell-viability test reagent. (left) a bright-field image. (right) a fluorescence image. Scale bars indicate 200μm.

Multiple trials of single-cell loading on a single microwell array may be expected to increase the throughput of single cell trapping. To investigate the effect of multiple single-cell loading and washing trials, cell-occupancies of individual microwells were monitored while repeating the identical single-cell trapping trials. Figure 5.6 shows the number of empty, single-cell-trapped, and multiple-cell-trapped microwells within a single microwell array chip along with the number of cell-trapping trials. The number of microwells with single-cell occupancy was found to be gradually decreased as the number of cell-trapping trials is increased. The number of empty microwells was also found to be decreased with the number of

single-cell-trapped microwells whereas the number of microwells with multiple cells increases with the number of trials, showing that the repetitive single-cell loading does not give higher single-cell occupancy in the given experimental conditions.

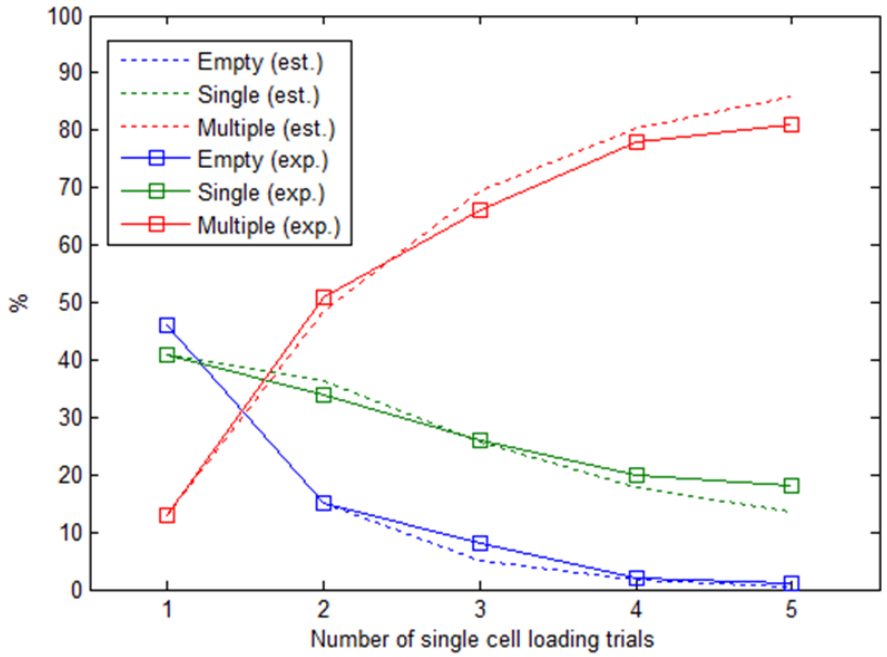

Figure 5.6 Effect of multiple single-cell loading trials on the microwell occupancies. Experiments were performed using a microwell array with a microwell diameter of ~ 15μm. Estimated occupancies were calculated from the first loading result and the empirical cell-trapping matrix.

To find out whether there is a general rule of single cell trapping trials, cell-occupancies of all the individual microwells were modeled and analyzed. A single cell-trapping trial can be described as

$$N_{m+1} = T_m N_m \tag{5.1}$$

where N_m is a 3 × 1 matrix with the number of empty, single-cell-trapped, and multiple-cell-trapped microwells and T_m is a 3 × 3 cell-trapping matrix with cell-trapping coefficients after m-th cell-trapping trial:

$$N_m = \begin{pmatrix} n_{empty,m} \\ n_{single,m} \\ n_{multiple,m} \end{pmatrix} \tag{5.2}$$

$$\text{and} \quad T_m = \begin{pmatrix} t_{E,E} & t_{S,E} & t_{M,E} \\ t_{E,S} & t_{S,S} & t_{E,S} \\ t_{E,M} & t_{S,M} & t_{M,M} \end{pmatrix}. \tag{5.3}$$

Here the cell-trapping coefficient $t_{i,j}$ indicates a probability in that microwells in the state i goes to the state j by m-th cell-trapping trial, where i and j can be E(empty), S(single-cell-trapped) or M(multiple-cell-trapped). From the experimental result a general cell-trapping matrix T was obtained as

$$T_m = T = \begin{pmatrix} 0.29 & 0.04 & 0 \\ 0.37 & 0.49 & 0.05 \\ 0.34 & 0.47 & 0.95 \end{pmatrix} \quad \text{for all } m \ (m \neq 1) \tag{5.4}$$

with an exception for the first cell-trapping trial:

$$T_1 = \begin{pmatrix} 0.46 & - & - \\ 0.41 & - & - \\ 0.13 & - & - \end{pmatrix}. \quad (5.5)$$

Based on the obtained cell-trapping matrix, several rules were commonly determined as following:

(iv) Once cells are trapped in microwells, those cells barely get out of the trapped microwells ($t_{S,E}$, $t_{M,E} < 0.05$).

(v) If multiple cells are trapped in a single microwell, most of them (~95%) remain in the microwell regardless of washing step.

(vi) The portion of empty microwells becoming occupied by single cells in the next step is ~ 37% ($t_{E,S}$) whereas that of single-cell-trapped microwells becoming occupied by multiple cells in the next step is ~ 47% ($t_{S,M}$), inferring that additional cell-loading trials will yield less single-cell-trapped microwells eventually.

From the obtained general cell-trapping matrix, a series of estimated cell-trapping results was obtained. The estimated cell-trapping results along with the number of cell-trapping trials were found to strongly agree with the experimental results (Figure 5.6).

5.2.3 Microwell Assembly

To isolate the trapped-cells into separate reaction chambers, the cell-trapped microwell array was assembled with the microwells having larger volumes. To provide precise alignment of assembly between two microwell array chips, a 4-axis (*X, Y, Z and θ*) translational stage was equipped onto a microscope stage. The position and orientation of the microwell array having large microwells were adjusted by controlling the 4-axis stage while a cell-trapped microwell array was loaded on a microscope stage. After finishing manual alignment of microwells, the two microwell arrays were assembled into a single microwell array by placing the chips close to each other.

To visualize the separation of reaction chambers, lysis of cells were tested using fluorescently-labeled cells. After labeling of cells using a cell viability test kit, viable cells show green fluorescence due to intracellular fluorescence molecules produced by cellular enzymatic reactions. The intracellular green fluorescence molecules spread out to its environments when cells are lysed. After assembled with detergent (0.1% NP-40)-containing microwells, the green fluorescence molecules, which were localized within cell-trapping microwells, were found to be spread throughout their paired-microwells (Figure 5.7). Adjacent microwells without trapped-cells were found to show no fluorescence intensity increase 20min after the microwell assembly.

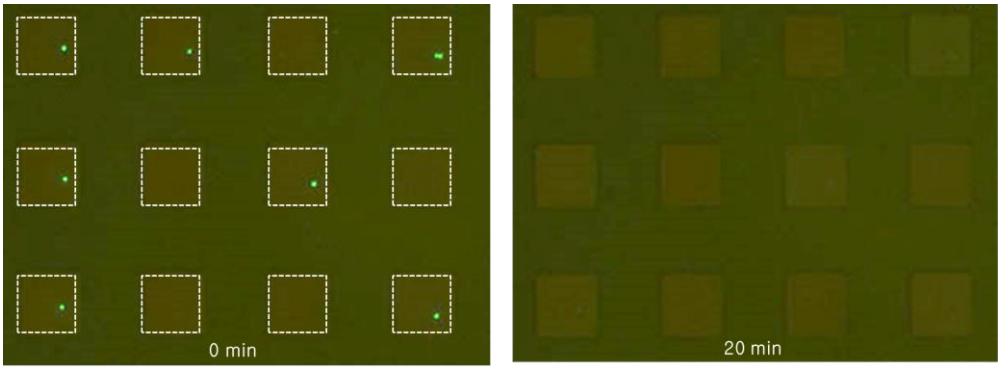

Figure 5.7 Localized spread of intracellular green fluorescence molecules into paired-microwells. After assembled with detergent-containing microwells, cells were lysed and the green fluorescence molecules were spread out to the microwells.

5.3 Single-Cell RT-qPCR

By combining a single-cell array formed on a multivolume microwell array with the 'one-pot' lysis-RT-PCR condition, microwell-based parallel single-cell RT-PCR was performed. Using the real-time on-chip PCR system, real-time amplification curves were obtained and used for quantitative analysis of various samples. Firstly, the thermocycling condition was adjusted to work with a PDMS-based multivolume microwell array. The integrated RT-qPCR system was then validated through standard curve analysis. Quantitative analysis of single cell gene expression was also performed using the system.

5.3.1 PCR Conditions for an Assembled Microwell Array

In this work a multivolume microwell array is constructed by assembling two microwell array microchips both of which are made of PDMS. As a result, whole microwells become enclosed by PDMS and the thickness of the PDMS microchip determines the distance of the microwells from the surface of a thermocycler. This microwell-to-thermocycler distance then determines the time required for the desired heat transfer characteristics. In addition, PDMS and glass differ in thermal properties and therefore the effective thermal distance between the microwells and the thermocycler surface becomes different even in the case of the same thickness. In short, a thermocycling condition for the multivolume microwell array needs to be

adjusted in order to compensate the change of heat transfer characteristics across the microchip.

To find the changes of the heat transfer characteristics induced by insertion of a single PDMS layer (a part of a multivolume microwell array), a temperature change at the microwell position was estimated using a finite element method (FEM) simulation tool (2D Heat Transfer by Conduction model, COMSOL Multiphysics). As a microchip heat transfer model, four neighboring rectangular blocks with the height of 1mm, 0.8mm, 3mm, and 50mm were assumed for a glass substrate, a PDMS block with cell trapping microwells, a PDMS block with reaction chamber microwells, and air as ambient environment, respectively (Figure 5.8). Using the microchip heat transfer model, temperature changes at the surface of the glass substrate and the surface of the cell trapping microwells were estimated for 60s under the temperature transition of 60˚C to 95˚C and 95˚C to 60˚C. The estimation result shows much slower temperature change at the PDMS surface than at the glass surface; within the first 10s, 90% of temperature transition is finished at the glass surface while at the PDMS surface only 37% of the transition is progressed (Figure 5.9).

Pre-defined thermocycling condition for small-volume on-chip PCR was also found to give no positive RT-PCR result when a multivolume microwell array was used, indirectly agreeing with the theoretical estimations. In order to compensate the

change of heat transfer characteristics across the microchip, modification of thermocycling condition was tried. After a series of modification trials, the thermocycling condition was adjusted to successfully reproduce the same RT-PCR results on a multivolume microwell array microchip.

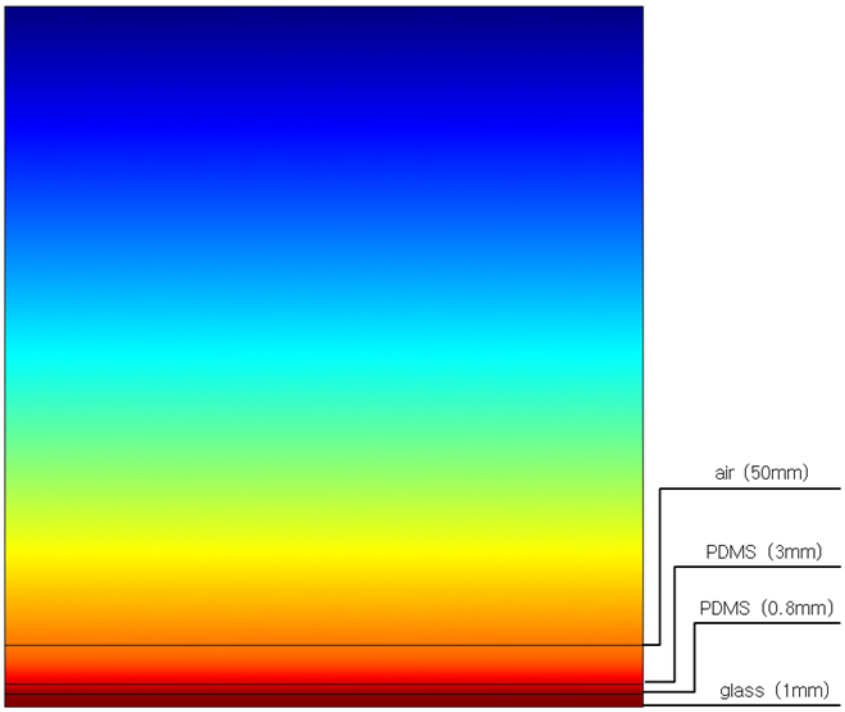

Figure 5.8 FEM simulation model for a multivolume microwell array microchip. The surface of thermocycler is assumed to be located at the bottom of the glass substrate.

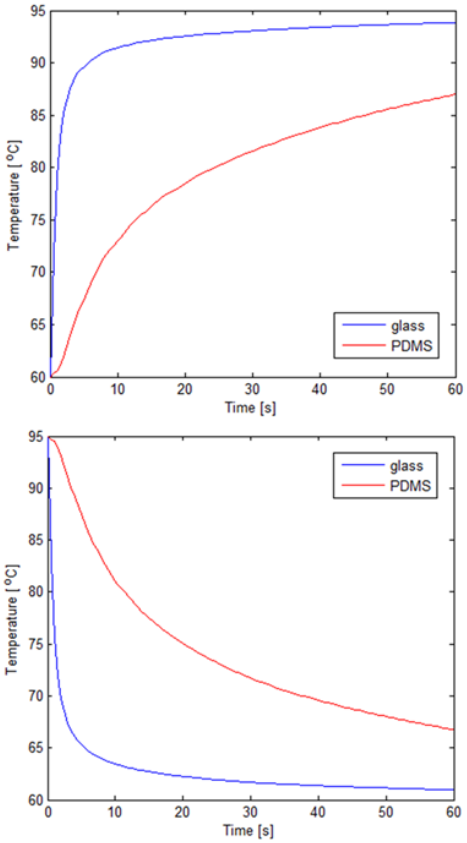

Figure 5.9 FEM simulation model for a multivolume microwell array microchip. The surface of thermocycler is assumed to be located at the bottom of the glass substrate. Constants in the model are as following: thermal conductivity of glass, PDMS and air ~ 1.38 W/(m·K), 0.15 W/(m·K) and ~ 0.024 W/(m·K), heat capacity of glass, PDMS and air ~ 703 J/(kg·K), 1500 J/(kg·K) and 1005 J/(kg·K), density of glass, PDMS and air ~ 2203 kg/m^3, 970 kg/m^3 and 1.2 kg/m^3.

5.3.2 Standard Curve Analysis

Before analyzing gene expression levels of single cells, a standard curve analysis was performed to obtain a quantification standard. For this total RNA sample was prepared from HL-60 cells using a commercial RNA extraction kit (Qiagen) and used as a RNA target standard. Figure 5.10 shows real-time amplification curves obtained from conventional 20μL RT-qPCR reactions with various total RNA concentrations. From the conventional RT-qPCR reactions threshold cycle (C_t) values were obtained to be 26.2, 29.4, 32.5 and 34.6 for sample RNA amount of 512pg, 64pg, 8pg and 1pg, respectively (CV < 2%). Under the assumption of 100% efficiency of reverse transcription, efficiency of PCR reaction in the conventional RT-qPCR was obtained to be 106.9% from standard curve analysis (Figure 5.11).

Microwell-based small-volume (~12.5nL) RT-qPCR reactions were also found to show similar real-time amplification curves with the conventional reactions (Figure 5.12). From microwell-based on-chip RT-qPCR reactions with various RNA concentrations (64pg, 8pg, 1pg and 0.125pg), the on-chip PCR efficiency of ~ 114.2% was obtained (Figure 5.13). In all RNA concentrations studied, the detection sensitivity was found to be improved in case of small-volume reactions as C_t values were lower in microwell environments than in conventional tube environments (average C_t deviation ~ 10.4).

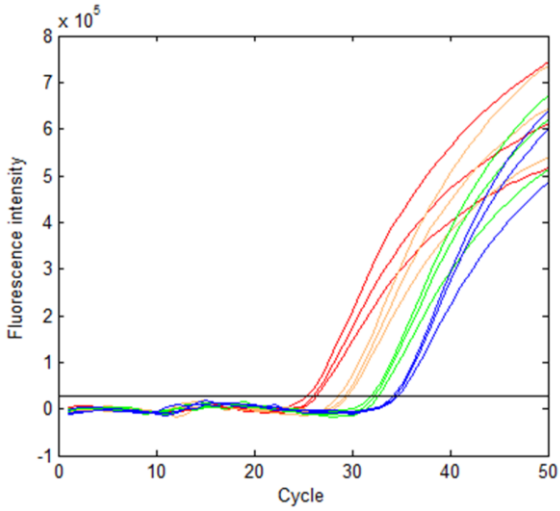

Figure 5.10 Real-time amplification curves obtained from conventional 20μL RT-qPCR reactions with various total RNA concentrations. (red) 512pg, (orange) 64pg, (green) 8pg, and (blue) 1pg. A black line indicates threshold cycles.

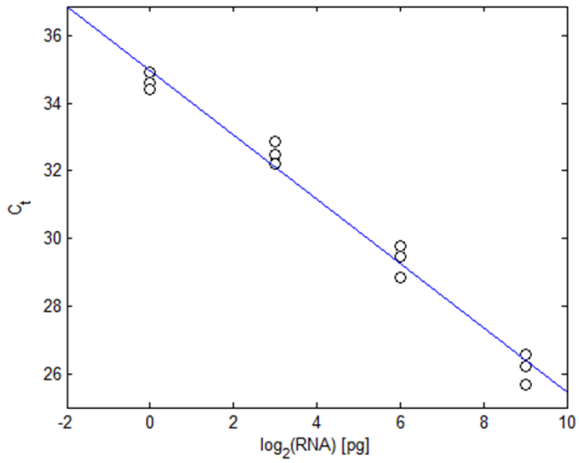

Figure 5.11 Standard curve analysis result using the real-time amplification curves in Figure 5.10. A blue line indicates a least-squares line from the all data points.

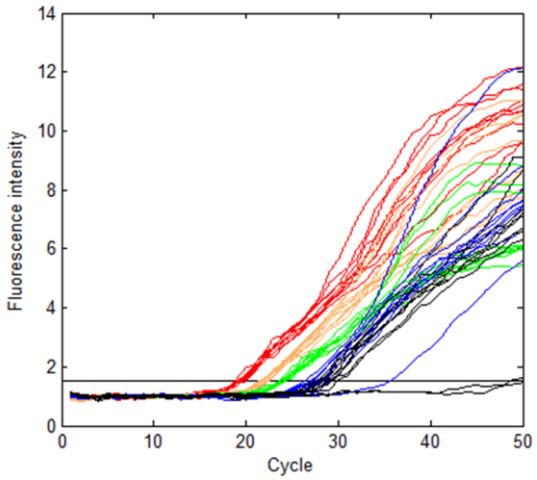

Figure 5.12 Real-time amplification curves obtained from microwell-based 12.5nL RT-qPCR reactions with various total RNA concentrations. (red) 64pg, (orange) 8pg, (green) 1pg, (blue) 0.125pg, and (gray) 15.625fg. A black line indicates threshold cycles.

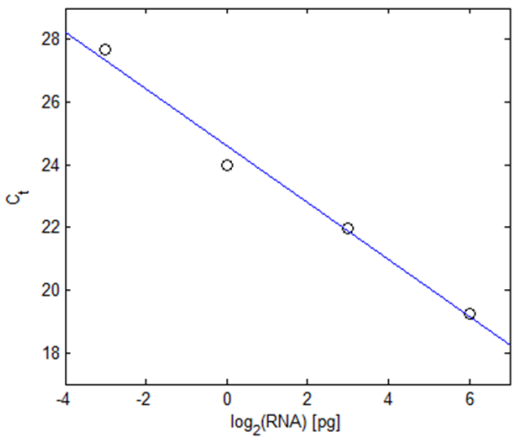

Figure 5.13 Standard curve analysis result using the real-time amplification curves in Figure 5.12. A blue line indicates a least-squares line from the all data points.

5.3.3 Single-Cell Gene Quantification

Using the standard curve analysis result quantification of single-cell gene expression was performed. In the mulitivolume microwell array experiment, NP-40 was not included in the final RT-PCR reagent mixture in order to suppress inter-well cross-contamination possibly caused by well-to-well transport of cellular RNA molecules. Instead, a sufficient cell-lysis time (~30min) was allowed after the microwell assembly; in this water-based reagent condition, cell membrane is expected to be lysed due to osmotic pressure. Figure 5.14 shows a multivolume microwell array with trapped single cells; here, live cells are stained with blue live-cell indicating reagent (Calcein Blue AM, Life Technologies). Amplification-specific signal (in green fluorescence channel) shows heterogeneous pattern after the thermocycling. The heterogeneous amplification distribution is expected to be originated from the heterogeneity of cell occupancies across the microwell array. Indeed, microwells with trapped single cells showed threshold cycles of ~23.0 while cell-free microwells showed no amplification. Some of the cell-free microwells showed unexpected amplifications; however, their threshold cycles were relatively high (~29.5), possibly showing the amplifications of single molecules (Figure 5.15). This result suggests that the isolated and crosstalk-free microwell RT-PCR reactions were successfully achieved.

Using the standard curve analysis result as a quantification standard, the

quantity of single-cell RNA is estimated to be ~3.36pg, which agrees with the literature very well [65]. The number of GAPDH molecules in a single cell can be estimated to be ~ 207 based on the following;

$$N_{SingleCell} = (1 + efficiency)^{C_t(SingleMolecule) - C_t(SingleCell)}. \qquad (5.6)$$

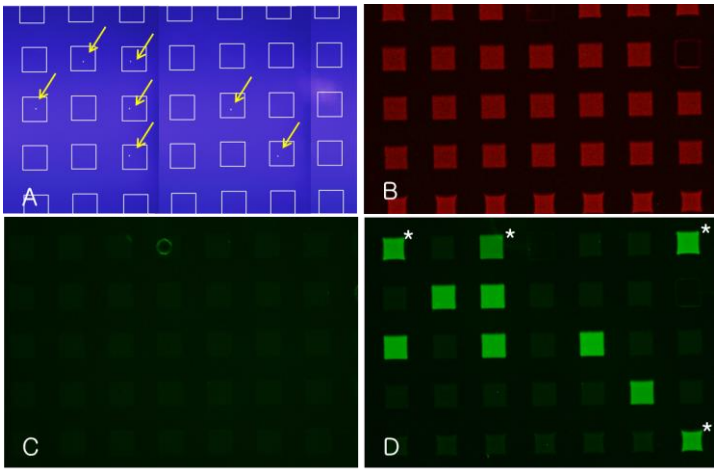

Figure 5.14 A multivolume microwell array for quantification of single-cell gene expression (A) An assembled microwell array with trapped single cells. Cells are indicated by yellow arrows. (B) A red fluorescence image showing the microwell positions. (C) A green fluorescence image before thermocycling. (D) A green fluorescence image after thermocycling. Some distinct signal amplifications in cell-free microwells were found to have relatively high threshold cycles (~29.5), possibly showing the amplifications of single molecules (denoted by asterisks).

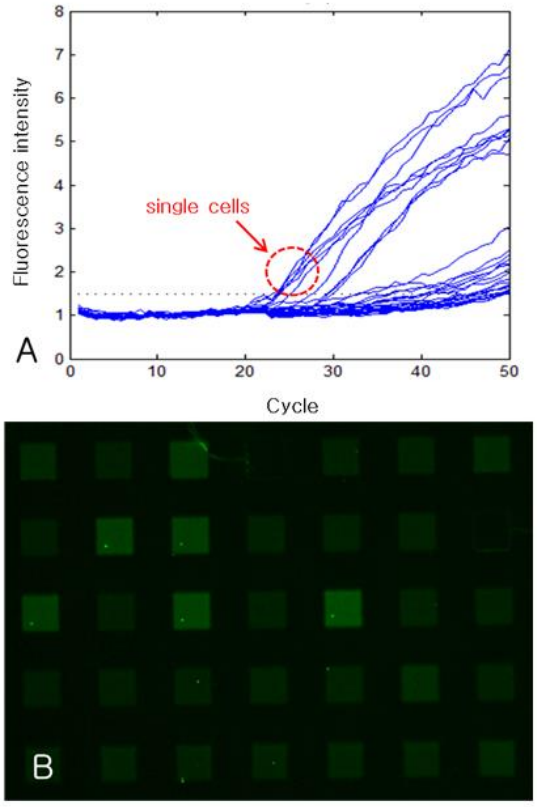

Figure 5.15 (A) Real-time amplification curves from a multivolume microwell array shown in Figure 5.14. (B) A green fluorescence image at the thermocycle number of 30.

5.4 Future Work: Single-Cell Transcriptome Analysis

In gene expression profiling technologies, the number of genes simultaneously analyzed is very important since understanding of complicated relations between interactive genes is required in many related applications such as a finding of a new genetic biomarker. RT-qPCR technologies rely on optical detection of gene-specific fluorescence signals and therefore, a number of different fluorescence reporters should be employed for multiplexed analyses. This technical drawback restricts the degree of multiplexity of RT-qPCR to a few genes at maximum.

In order to fully appreciate the cellular information on gene expression levels as well as genetic mutative events, recently-developed DNA sequencing technologies are considered as the best candidate since all the genetic information can be read at the level of single base resolutions. Recently, single cell transcriptome analysis, which was achieved by the acquisition of the whole single cell mRNA followed by sequencing of acquired transcripts, was demonstrated [62, 63]. The sequencing-based gene expression profiling is a very promising method compared to PCR-based methods because the expression levels of all genes are simultaneously obtained and analyzed in an interactive manner, making the interactive behavior of multiple gene expressions more comprehensible. For now, the only drawback of the sequencing-based analysis is its extremely high cost.

The multivolume microwell array technology is expected to serve as a simple

and low-cost single-cell RT-qPCR system. Despite of its capability of analyzing single cell gene expressions in a quantitative manner, it has the same technical limitations as the other RT-qPCR approaches including single-cell RT-qPCR. To obtain an expanded technical capability for whole transcriptome analysis, the microwell-based approaches need to be further improved; one good candidate approach is to provide a technical interface with DNA sequencing technologies. One method enabling transcriptome analysis of multiple single cells in a highly-parallelized manner would serve as a powerful method for low-cost and parallelized single cell transcriptome analysis.

To apply the multivolume microwell array technology to single cell transcriptome analysis, a technical handling for differentiating information of individual single cells is essentially required. In single cell sequencing applications, single cell DNA-tagging approach is usually applied to store information for single cell identifications [66]. In those applications, massive sequencing data are rearranged based on the DNA tag information which identifies the source cell of the sequencing reads. The microwell structure is also expected to be used for single cell tagging in combination with the use of microwell-specific tag information. The microwell-specific (i.e. single-cell-specific) tagging can be easily realized by the use of a DNA microarray. To be more specific, the spatial distribution of DNA oligonucleotide tag information on a DNA microarray is designed to correspond

closely with the spatial distribution of cell-trapping microwells (Figure 5.16). In this configuration, individual single cells trapped in the microwells are exposed to microwell-specific DNA having different tag information. By attaching microwell-specific tag information on the RNA transcripts from individual single cells, single-cell whole transcriptome tagging can be achieved. The sequencing sample can then be prepared through a series of biochemical reactions including RT-PCR (Figure 5.17). This microwell-based approach is expected to enable parallelized single-cell transcriptome analysis in high throughput. In addition, those parallelized analysis with low analysis cost will be further advanced toward single-cell-based diagnosis in medicinal biology (Figure 5.18).

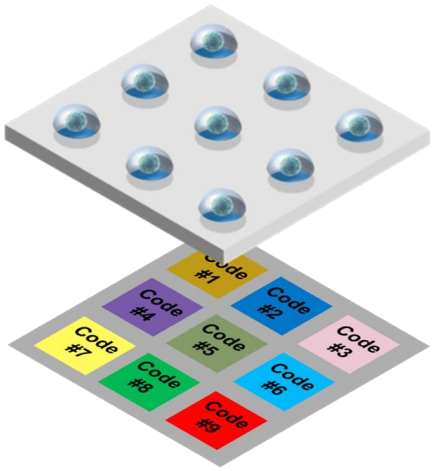

Figure 5.16 A concept of single cell tagging using a microwell array and a DNA microarray.

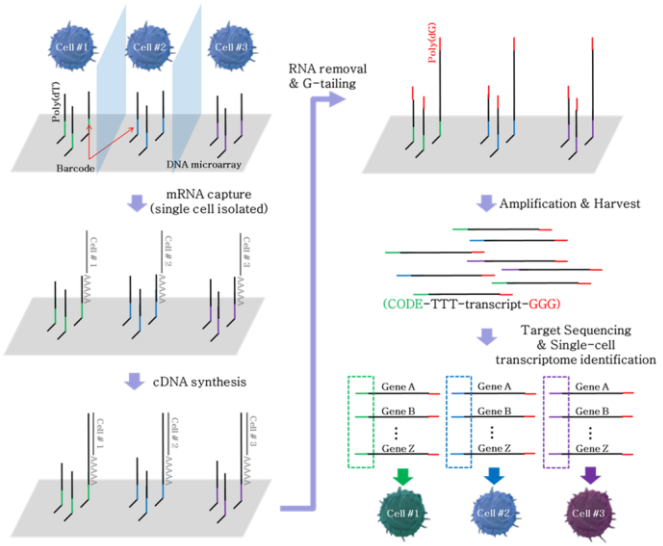

Figure 5.17 A concept of parallel single cell transcriptome analysis.

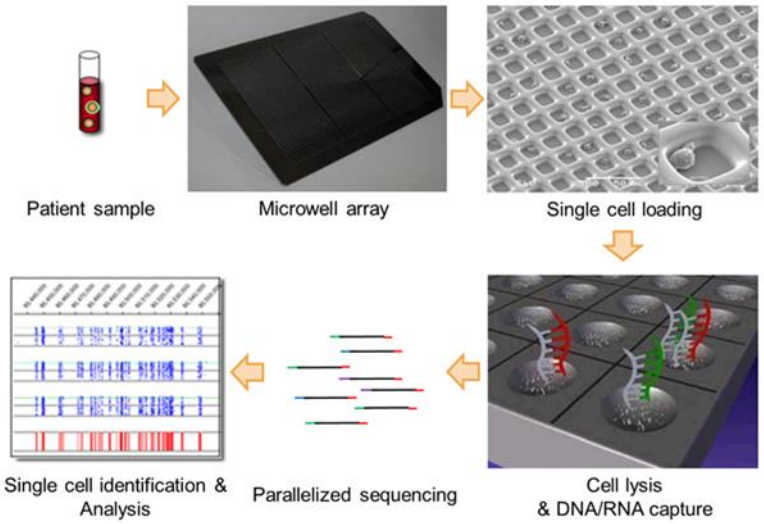

Figure 5.18 A concept of diagnosis applications based on single cell sequencing

Chapter 6

Conclusion

A concept of multivolume microwell array approach was proposed for the purpose of realization of quantitative single-cell gene expression analysis. In the multivolume microwell array approach, two microwell arrays with different microwell volumes were assembled into a single microwell array with volume-adjusted microwells. This volume adjustment of microwells was applied to parallelized single-cell trapping followed by reaction volume dilution. The microwell-based single cell dilution technique was utilized for the realization of microwell-based single cell RT-qPCR, which requires a sufficient dilution of cell lysate for reproduction of the reliable result.

To realize the development of single-cell RT-qPCR system, several technical

challenges were identified and resolved. Firstly, small-volume on-chip PCR system based on the microwell technology was achieved (Chapter 3). For this, several elemental technologies were developed and they include preparation of microwell arrays and development of real-time on-chip PCR monitoring system. Secondly, ‘one-pot’ lysis-RT-PCR condition was obtained (Chapter 4). By setting an inhibition-free single-volume RT-PCR reagent preparation condition, RT-PCR product was found to be reliably obtained from intact cell samples as an amplification target. Integration of individually-developed achievements was finally achieved to realize a quantitative gene expression analysis system (Chapater 5). The obtained RT-qPCR system with the reaction volume of ~12.5nL reproduced similar RT-qPCR result with an improved sensitivity and throughput, compared to the conventional large volume (~20μL) RT-qPCR reaction settings. In combination with the multivolume microwell array providing single-cell trapping and subsequent dilution of its lysate, single-cell RT-qPCR was successfully performed without the reaction inhibition by cell lysate. Based on the single cell analysis result with a standard analysis data for quantification, gene expression level of single cells was analyzed in a quantitative manner.

The achieved system is expected to serve as a quantitative analysis system for single-cell gene expression profiling with low cost and high throughput. The microwell-based single cell analysis platform is also expected to be further

improved toward single-cell whole transcriptome analysis in combination with the use of DNA microarray technology and DNA sequencing technologies.

Bibliography

[1] H. Kortmann, L. M. Blank, and A. Schmid, “Single Cell Analytics: An Overview,” *Advances in Biochemical Engineering / Biotechnology*, vol. 124, pp. 99-122, 2011.

[2] D. Ryan, K. Ren, and H. Wu, “Single-cell assays,” *Biomicrofluidics*, vol. 5, pp. 021501, 2011.

[3] Y. Lin, R. Trouillon, G. Safina et al., “Chemical Analysis of Single Cells,” *Analytical Chemistry*, vol. 83, pp. 4369-4392, 2011.

[4] M. Wu and A. K. Singh, “Single-cell protein analysis,” *Current Opinion in Biotechnology*, vol. 23, pp. 83-88, 2012.

[5] T. Kalisky and S. R. Quake, “Single-cell genomics,” *Nature Methods*, vol. 8, pp. 311-314, 2011.

[6] D. Wang and S. Bodovitz, “Single cell analysis: the new frontier in ‘omics’,” *Trends in Biotechnology*, vol. 28, pp. 281-290, 2010.

[7] *http://en.wikipedia.org/wiki/Micromanipulator*

[8] *http://microscope.olympus-global.com/en/ga/product/on3/*

[9] W. A. Bonner, H. R. Hulett, R. G. Sweet et al., "Fluorescence Activated Cell Sorting," *Review of Scientific Instruments*, vol. 43, pp. 404-409, 1972.

[10] L. A. Herzenberg, D. Parks, B. Sahaf et al., "The History and Future of the Fluorescence Activated Cell Sorter and Flow Cytometry: A View from Stanford," *Clinical Chemistry*, vol. 48, pp. 1819-1827, 2002.

[11] R. N. Zare and S. Kim, "Microfluidic Platforms for Single-Cell Analysis," *Annual Review of Biomedical Engineering*, vol. 12, pp. 187-201, 2010.

[12] S. Lindström and H. Andersson-Svahn, "Overview of single-cell analyses: microdevices and applications," *Lab on a Chip*, vol. 10, pp. 3363-3372, 2010.

[13] H. Andersson and A. van den Berg, "Microtechnologies and nanotechnologies for single-cell analysis," *Current Opinion in Biotechnology*, vol. 15, pp. 44-49, 2004.

[14] H. N. Joensson and H. Andersson-Svahn, “Droplet Microfluidics—A Tool for Single-Cell Analysis,” *Angewandte Chemie International Edition*, vol. 51, pp. 12176-12193, 2012.

[15] T. D. Chung and H. C. Kim, “Recent advances in miniaturized microfluidic flow cytometry for clinical use,” *Electrophoresis*, vol. 28, pp. 4511-4520, 2007.

[16] D. Huh, W. Gu, Y. Kamotani et al., “Microfluidics for flow cytometric analysis of cells and particles,” *Physiological Measurement*, vol. 26, pp. R73-R98, 2005.

[17] T. Sun and H. Morgan, “Single-cell microfluidic impedance cytometry: a review,” *Microfluidics and Nanofluidics*, vol. 8, pp. 423-443, 2010.

[18] M. Schena, D. Shalon, R. W. Davis et al., “Quantitative Monitoring of Gene Expression Patterns with a Complementary DNA Microarray,” *Science*, vol. 270, pp. 467-470, 1995.

[19] A. A. Alizadeh, M. B. Eisen, R. E. Davis et al., “Distinct types of diffuse large B-cell lymphoma identified by gene expression profiling,” *Nature*, vol. 403, pp. 503-511, 2000.

[20] C. M. Perou, T. Sørlie, M. B. Eisen et al., “Molecular portraits of human breast tumours,” *Nature*, vol. 406, pp. 747-752, 2000.

[21] T. Sørlie, C. M. Perou, R. Tibshirani et al., “Gene expression patterns of breast carcinomas distinguish tumor subclasses with clinical implications,” *Proceedings of the National Academy of Sciences of the United States of America*, vol. 98, pp. 10869-10874, 2001.

[22] K. Kurimoto, Y. Yabuta, Y. Ohinata et al., “An improved single-cell cDNA amplification method for efficient high-density oligonucleotide microarray analysis,” *Nucleic Acids Research*, vol. 34, pp. e42, 2006.

[23] C. A. Klein, S. Seidl, K. Petat-Dutter et al., “Combined transcriptome and genome analysis of single micrometastatic cells,” *Nature Biotechnology*, vol. 20, pp. 387-392, 2002.

[24] T. Nolan, R. E. Hands, and S. A. Bustin, “Quantification of mRNA using real-time RT-PCR,” *Nature Protocols*, vol. 1, pp. 1559-1582, 2006.

[25] H. D. VanGuilder, K. E. Vrana, and W. M. Freeman, “Twenty-five years of quantitative PCR for gene expression analysis,” *BioTechniques 25th Anniversary*, vol. 44, pp. 619-626, 2008.

[26] C. A. Heid, J. Stevens, K. J. Livak et al., “Real Time Quantitative PCR,” *Genome Research*, vol. 6, pp. 986-994, 1996.

[27] A. Giulietti, L. Overbergh, D. Valckx et al., “An Overview of Real-Time Quantitative PCR: Applications to Quantify Cytokine Gene Expression,” *Methods*, vol. 25, pp. 386-401, 2001.

[28] O. Kalinina, I. Lebedeva, J. Brown et al., “Nanoliter scale PCR with TaqMan detection,” *Nucleic Acids Research*, vol. 25, pp. 1999-2004, 1997.

[29] B. Vogelstein and K. W. Kinzler, “Digital PCR,” *Proceedings of the National Academy of Sciences of the United States of America*, vol. 96, pp. 9236-9241, 1999.

[30] *http://www.fluidigm.com/rt-digital-pcr.html*

[31] M. L. Metzker, “Sequencing technologies — the next generation,” *Nature Reviews Genetics*, vol. 11, pp. 31-46, 2010.

[32] M. Margulies, M. Egholm, W. E. Altman et al., “Genome sequencing in microfabricated high-density picolitre reactors,” *Nature*, vol. 437, pp. 376-380, 2005.

[33] D. R. Bentley, S. Balasubramanian, H. P. Swerdlow et al., “Accurate whole human genome sequencing using reversible terminator chemistry,” *Nature*, vol. 456, pp. 53-59, 2008.

[34] A. Valouev, J. Ichikawa, T. Tonthat et al., “A high-resolution, nucleosome position map of C. elegans reveals a lack of universal sequence-dictated positioning,” *Genome Research*, vol. 18, pp. 1051-1063, 2008.

[35] T. D. Harris, P. R. Buzby, H. Babcock et al., “Single-Molecule DNA Sequencing of a Viral Genome,” *Science*, vol. 320, pp. 106-109, 2008.

[36] J. Eid, A. Fehr, J. Gray et al., “Real-Time DNA Sequencing from Single Polymerase Molecules,” *Science*, vol. 323, pp. 133-138, 2009.

[37] R. Drmanac, A. B. Sparks, M. J. Callow et al., "Human Genome Sequencing Using Unchained Base Reads on Self-Assembling DNA Nanoarrays," *Science*, vol. 327, pp. 78-81, 2010.

[38] J. M. Rothberg, W. Hinz, T. M. Rearick et al., "An integrated semiconductor device enabling non-optical genome sequencing," *Nature*, vol. 475, pp. 348-352, 2011.

[39] Z. Wang, M. Gerstein, and M. Snyder, "RNA-Seq: a revolutionary tool for transcriptomics," *Nature Reviews Genetics*, vol. 10, pp. 57-63, 2009.

[40] B. T. Wilhelm and J.-R. Landry, "RNA-Seq—quantitative measurement of expression through massively parallel RNA-sequencing," *Methods*, vol. 48, pp. 249-257, 2009.

[41] F. Ozsolak and P. M. Milos, "RNA sequencing: advances, challenges and opportunities," *Nature Reviews Genetics*, vol. 12, pp. 87-98, 2011.

[42] U. Nagalakshmi, Z. Wang, K. Waern et al., "The Transcriptional Landscape of the Yeast Genome Defined by RNA Sequencing," *Science*, vol. 320, pp. 1344-1349, 2008.

[43] F. Ozsolak, A. R. Platt, D. R. Jones et al., “Direct RNA sequencing,” *Nature*, vol. 461, pp. 814-819, 2009.

[44] E. A. Ottesen, J. W. Hong, S. R. Quake et al., “Microfluidic Digital PCR Enables Multigene Analysis of Individual Environmental Bacteria,” *Science*, vol. 314, pp. 1464-1467, 2006.

[45] K. A. Heyries, C. Tropini, M. VanInsberghe et al., “Megapixel digital PCR,” *Nature Methods*, vol. 8, pp. 649-651, 2011.

[46] A. C. Hatch, J. S. Fisher, A. R. Tovar et al., “1-Million droplet array with wide-field fluorescence imaging for digital PCR,” *Lab on a Chip*, vol. 11, pp. 3838-3845, 2011.

[47] F. Shen, W. Du, J. E. Kreutz et al., “Digital PCR on a SlipChip,” *Lab on a Chip*, vol. 10, pp. 2666-2672, 2010.

[48] F. Moltzahn, A. B. Olshen, L. Baehner et al., “Microfluidic-Based Multiplex qRT-PCR Identifies Diagnostic and Prognostic microRNA Signatures in the Sera of Prostate Cancer Patients,” *Cancer Research*, vol. 71, pp. 550-560, 2011.

[49] F. Shen, W. Du, E. K. Davydova et al., “Nanoliter Multiplex PCR Arrays on a SlipChip,” *Analytical Chemistry*, vol. 82, pp. 4606-4612, 2010.

[50] F. Shen, B. Sun, J. E. Kreutz et al., “Multiplexed Quantification of Nucleic Acids with Large Dynamic Range Using Multivolume Digital RT-PCR on a Rotational SlipChip Tested with HIV and Hepatitis C Viral Load,” *Journal of the American Chemical Society*, vol. 133, pp. 17705-17712, 2011.

[51] Z. Hua, J. L. Rouse, A. E. Eckhardt et al., “Multiplexed Real-Time Polymerase Chain Reaction on a Digital Microfluidic Platform,” *Analytical Chemistry*, vol. 82, pp. 2310-2316, 2010.

[52] A. K. White, M. VanInsberghe, O. I. Petriv et al., “High-throughput microfluidic single-cell RT-qPCR,” *Proceedings of the National Academy of Sciences of the United States of America*, vol. 108, pp. 13999-14004, 2011.

[53] V. Sanchez-Freire, A. D. Ebert, T. Kalisky el al., “Microfluidic single-cell real-time PCR for comparative analysis of gene expression patterns,” *Nature Protocols*, vol. 7, pp. 829-838, 2012.

[54] J. C. Love, J. L. Ronan, G. M. Grotenbreg et al., "A microengraving method for rapid selection of single cells producing antigen-specific antibodies," *Nature Biotechnology*, vol. 24, pp. 703-707, 2006.

[55] A. Jin, T. Ozawa, K. Tajiri et al., "A rapid and efficient single-cell manipulation method for screening antigen-specific antibody-secreting cells from human peripheral blood," *Nature Medicine*, vol. 15, pp. 1088-1092, 2009.

[56] D. K. Wood, D. M. Weingeist, S. N. Bhatia et al., "Single cell trapping and DNA damage analysis using microwell arrays," *Proceedings of the National Academy of Sciences of the United States of America*, vol. 107, pp. 10008-10013, 2010.

[57] J. Hoffmann, M. Trotter, F. von Stetten et al., "Solid-phase PCR in a picowell array for immobilizing and arraying 100000 PCR products to a microscope slide," *Lab on a Chip*, vol. 12, pp. 3049-3054, 2012.

[58] Y. Gong, A. O. Ogunniyi, and J. C. Love, “Massively parallel detection of gene expression in single cells using subnanolitre wells,” *Lab on a Chip*, vol. 10, pp. 2334-2337, 2010.

[59] B. J. DeKosky, G. C. Ippolito, R. P. Deschner et al., “High-throughput sequencing of the paired human immunoglobulin heavy and light chain repertoire,” *Nature Biotechnology*, vol. 31, pp. 166-169, 2013.

[60] Y. Xia and G. M. Whitesides, “SOFT LITHOGRAPHY,” *Annual Review of Materials Science*, vol. 28, pp. 153-184, 1998.

[61] K. Kurimoto, Y. Yabuta, Y. Ohinata et al., “Global single-cell cDNA amplification to provide a template for representative high-density oligonucleotide microarray analysis,” *Nature Protocols*, vol. 2, pp. 739-752, 2007.

[62] F. Tang, C. Barbacioru, Y. Wang et al., “mRNA-Seq whole-transcriptome analysis of a single cell,” *Nature Methods*, vol. 6, pp. 377-382, 2009.

[63] F. Tang, C. Barbacioru, E. Nordman et al., "RNA-Seq analysis to capture the transcriptome landscape of a single cell," *Nature Protocols*, vol. 5, pp. 516-535, 2010.

[64] J. R. Rettig and A. Folch, "Large-Scale Single-Cell Trapping And Imaging Using Microwell Arrays," *Analytical Chemistry*, vol. 77, pp. 5628-5634, 2005.

[65] F. Mollinedo, M. J. Vaquerizo, and J. R. Naranjo, "Expression of c-*jun*, *jun* B and *jun* D proto-oncogenes in human peripheral-blood granulocytes," *Biochemical Journal*, vol. 273, pp. 477-479, 1991.

[66] S. Islam, U. Kjällquist, A. Moliner et al., "Characterization of the single-cell transcriptional landscape by highly multiplex RNA-seq," *Genome Research*, vol. 21, pp. 1160-1167, 2011.

국문 초록

본 논문에서는 단일 세포 유전자 발현의 정량분석을 위한 다중적 부피를 갖는 미세우물구조 기반의 접근법을 제안하고 이를 구현한다. 세포는 모든 살아있는 생명체의 구조적, 기능적인 가장 기본적인 단위로서 다양하고 복잡한 생명현상의 본질을 이해하기 위한 가장 기초적인 요소이다. 수많은 복잡한 생명현상들이 세포들의 기작 및 세포간 혹은 세포와 외부 환경간의 상호작용에 의해 이루어지는 데 반해, 분자 생물학 및 세포 생물학 분야의 대부분의 연구는 수많은 세포들의 집단적인 평균적 겉보기 활동에 대한 관찰 및 해석에 의해 이루어져 왔다. 이는 기존의 전통적인 세포 분석 방법들의 기술적 수준의 한계에 따른 것인데, 세포의 생명활동과 관련하는 여러 가지 현상에 대한 보다 정확한 관찰 및 분석이 요구됨에 따라 기존에 이루어져 왔던 연구 방법들을 단일 세포 단위로 접근할 수 있는 진보된 기술의 필요성이 점차적으로 증가하고 있다.

다양한 종류의 분자 생물학적 분석법 가운데 본 연구에서는 유전자 정량 분석에 주목하였다. 유전자 세포 내 유전자 발현량은 세포의 기능적 활동을 결정짓는 단백질 발현과 직접적인 관련성을 가지기 때문에 세포의 생명 현상적

상태를 파악 하는 데에 주요 지표로 활용될 수 있다. 또한 하나의 생명체를 이루는 수많은 세포들이 거의 동일한 유전체 정보를 가지는 데에 반해 유전자 발현량은 내·외부적 환경에 따라 세포마다 다르게 나타나기 때문에 단일 세포 단위의 분석이 특히 요구된다.

최근 반도체 미세 공정 및 바이오칩 기술이 발전함에 따라 기존의 유전자 정량 분석법들로는 수행하기가 어려웠던 단일 세포 단위의 유전자 정량분석의 가능성을 높이는 기술들이 조금씩 개발되고 있다. 본 논문에서는 미세우물구조를 기반으로 하는 단일 세포 유전자 정량 기술의 개발에 대한 연구를 진행하였다. 즉, 각 미세우물구조 안에 단 하나의 세포만이 들어가게끔 유도한 후 미세우물구조들을 공간적으로 분리시킴으로써 수많은 독립적인 유전자 정량 반응을 병렬적으로 얻어내는 기술에 대하여 연구하였다.

미세우물구조 기반의 단일 세포 유전자 정량 분석을 이루어 내기에 앞서 두 가지 기술적인 어려움이 우선적으로 극복되었다. 우선 미세유체소자 기반의 유전자 정량 분석 환경을 구축하였다. 수많은 미세우물구조를 포함하는 미세유체소자를 제작하고, 미세유체 환경에서 유전자 증폭 반응을 성공적으로 재현하였다. 또한 유전자 정량 분석을 수행할 수 있는 실시간 유전자 증폭 분석계를 구현하였다. 다음으로 세포의 분쇄과정과 유전자 역전사 및 증폭과정이 단일 반응공간에서 연속적으로 이루어질 수 있는 시약 조성을 확보하였다. 별도의 유전자 추출과정 없이 세포를 반응에 첨가 하였을 때 유전자 역전사 및 증폭과정에 관여하는 효소 등의 기능을 손상시키지 않으면서 세포로부터 유전자

전사물을 획득하는 시약 조건을 확립함으로써 여러 단계에 걸쳐 이루어지는 세포 내 유전자 증폭 과정을 단일 반응공간에서 이루어 내었다.

단일 세포로부터의 유전자 획득 및 증폭이 안정적으로 이루어질 수 있는 반응 환경을 구축하기 위하여 서로 다른 부피를 갖는 두 미세우물구조를 하나로 합치는 방식의 접근법을 고안하여 연구를 진행하였다. 즉, 단일 세포와 비슷한 크기를 갖는 미세우물구조를 준비하여 단일 세포들을 가둔 후에 더 큰 부피를 갖는 미세우물구조와 대응시켜 결합함으로써 각각의 단일 세포들이 필요로 하는 부피의 반응 조건에 노출될 수 있도록 유도하였다. 이와 같은 미세우물구조 기반의 단일 세포 배치 방법을 미세유체환경의 실시간 유전자 증폭 분석법 및 단일 반응공간 세포 유전자 증폭 조건과 결합함으로써 하나의 미세유체소자에서 병렬적인 단일 세포 유전자 정량 분석을 성공적으로 수행하였다.

본 연구를 통해 얻어진 단일 세포 유전자 정량분석 기술은 높은 수율과 낮은 단가의 단일 세포 유전자 정량분석을 가능케 할 것으로 기대 된다. 또한 유전자 염기서열 분석기술과 결합되어 단일 세포 전사체 염기서열 분석 등의 기술로 발전될 수 있을 것이다.

주요어 : 단일 세포 분석, 유전자 정량 분석, 미세우물구조 어레이, 유전자 발현 프로파일링, 전사체 해석

학번 : 2007-23016